Power Pulsation Reduction Analysis in Dynamic Wireless Charging of Electric Vehicles

Azamat Mukhatov, Electrical and Electronics B.Eng

Submitted in fulfilment of the requirements for the degree of Master of Science in Electrical and Computer Engineering

School of Engineering Department
Electrical and Computer Engineering
Nazarbayev University

53 Kabanbay Batyr Avenue,
Astana, Kazakhstan, 010000

Supervisor: Mehdi Bagheri
Co-supervisor: Alexander Ruderman

2018

DECLARATION

I hereby, declare that this manuscript, entitled “Power Pulsation Reduction Analysis in Dynamic Wireless Charging of Electric Vehicles”, is the result of my own work except for quotations and citations which have been duly acknowledged.

I also declare that, to the best of my knowledge and belief, it has not been previously or concurrently submitted, in whole or in part, for any other degree or diploma at Nazarbayev University or any other national or international institution.

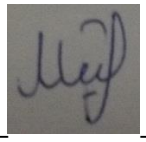

Name: Azamat Mukhatov

Date: 13.12.2018

Abstract

It is possible to considerably decrease the fossil fuel consumption and reduce the pollution created by the conventional vehicles by employing Electric Vehicles (EVs) and wireless charging techniques. The EV wireless charging systems can be divided into two categories based on the vehicle's position during charging, namely, Stationary Wireless Charging (SWC) and Dynamic Wireless Charging (DWC). DWC has more advantages as compared to SWC, in terms of charging time and reducing battery's size. Despite of the fact that it provides more benefits, there are various issues related to the passenger safety and the system's efficiency due to the fact that the vehicle is charged in motion. In addition, the issue of pulsations at the receiving coil mounted on the vehicle presents a significant challenge. Hence, this thesis specifically focuses on, discusses and analyzes the effect of distance between the adjacent transmitting coils, shape of the coils and distance between the transmitting as well as the receiving coils on the DWC system's output. In this thesis, mathematical modeling of a multi-channel DWC system is conducted, simulation and experimental studies for different distances between the transmitting coils are performed, and the results are discussed in detail. A possible solution to reduce the pulsations is provided and a future work on the subject of DWC systems for EVs is discussed. Moreover, the issue related to the electromagnetic safety of the system is considered and studied by means of a simulating the magnetic flux density around the coils.

Acknowledgements

I would like to express my special thanks of gratitude to Professor Mehdi Bagheri and Professor Alexander Ruderman for their extraordinary guidance, expert advice and help in writing this thesis.

I would also like to thank my family and friends for continuous support and encouragement throughout this project.

List of Publications

1. A. Mukhatov, M. Lu, M. Bagheri, M. S. Naderi and A. Nasiri, "A Practical Study on Output Power Pulsation Reduction in Dynamic Wireless Charging of Electric Vehicle," *Electrical Power Components and Systems, 2018.* (Submitted)

2. A. Mukhatov, M. Bagheri, P. Dehghanian, V. Carabias and G.B. Gharehpetian "Reduction of Output Power Pulsations for Electric Vehicles by Changing Distances between Transmitter Coils," *2018 ICRERA* (Published)

3. A.Mukhatov and M. Bagheri, "Behavior of Magnetic Flux Density in Dynamic Wireless Charging of Electric Vehicles", 2018 (Prepared)

4. M. Bagheri, A. Mukhatov, O.Abedinia, M.S.Naderi, M.S.Naderi and N.Ghadimi, "Application and Design of New Controller Based on Fuzzy PID and FACTS Devices in Multi-machine Power System," *2018 IEEE Int. Conf. Environ. Electr. Eng. 2018 IEEE Ind. Commer. Power Syst. Eur. (EEEIC / I&CPS Eur.*, pp. 1–6, 2018. (Published)

Table of Contents

List of Figures

List of Tables

Chapter 1 – Introduction

1.1 Background

Nowadays, dramatic degradation of the environment is the consequence of the significant amount of pollution produced by conventional vehicles. Moreover, intensive depletion of fossil fuels encourages international scientific and engineering community to investigate an alternative for conventional vehicles with internal combustion engines [1]–[5]. Therefore, different electric vehicles, namely Battery Electric Vehicles (BEV), Hybrid Electric Vehicles (HEV), Fuel Cell Electric Vehicles (FCEV) and Fuel Cell Hybrid Vehicles (FCHV), have been recommended to address the problem [1], [6], [7], [59]. Despite the fact that the pollution problem has been partially mitigated by these feasible solutions, hybrid vehicles are not widely used due to their main disadvantages related to the battery, such as its large size and long charging time [1], [8], [36]. In order to address these problems, a wireless charging technique is recommended [50], [51]. Wireless charging technique or Wireless Power Transfer (WPT) is a transmission of electrical power from a source to a load without a physical connector [6]. It can be divided into two classes, namely static and dynamic charging systems [9]. Both of the methods transfer power without employing charging cords, which ensures safety, isolation of power and reliability [10], [11], [45]. The main difference among them is that in case of the Static Wireless Charging (SWC) the power is transferred via a transmitting and receiving coils, which are both

stationary [46]. On the other hand, in case of Dynamic Wireless Charging (DWC) the transmitter is stationary, while the receiver is in motion [1], [12]–[15]. The main advantage of the Electric Vehicles (EVs) utilizing DWC, compared to those using SWC technique is that their battery can be charged while in motion [58],[60]. This, in turn, means that there is no idle time, and longer travelling distance can be achieved [42], [43]. Moreover, people usually charge their EV overnight during off-peak periods, which creates overloading of the network. Therefore, charging vehicles using DWC system will prevent network overloading and voltage excursions due to redistribution of load to different periods of time [62]. In addition, a smaller battery can potentially be employed, due to the fact that the energy is available on the road [16]. The method named inductive coupling is utilized to charge EVs under this concept. It allows transferring electrical energy between the coils via an oscillating magnetic field [17], [18], [33], [52]. Precisely, a primary or transmitting coil positioned at some distance from and magnetically coupled to a secondary or receiving coil can induce a certain voltage into it wirelessly [47]. Thus, the electric vehicle equipped with such system can be charged in motion without any cables [19]. However, the main limitation of the dynamic wireless charging system is the efficiency of the power transfer, which is significantly reduced by the fact that the charging procedure happens in dynamic circumstances. In other words, a constant lateral misalignment between the coils compromises the power transfer's efficiency

[1]–[3], [55]. This misalignment occurs due to the fact that as the EV moves along the road, its receiving coil installed under the cabin is constantly changing position with respect to the transmitting coils embedded into the road's track [56]. This phenomenon significantly degrades the quality of the received signal at the secondary side. Precisely, the induced voltage is not ideally constant, but experiences significant fluctuations in amplitude. This in turn affects the system's efficiency and reduces the battery's lifetime. Other factors affecting efficiency include the material used to manufacture the coils, which should not produce significant losses and should be able to carry provided amount of current without deteriorating the overall system's performance. In addition, the shape of the coils plays considerable role in forming their self and mutual inductances, which in turn has a direct effect on the efficiency [20]. Moreover, relative position of the coils on the track is also important [48]. In other words, large spacing between the coils reduces the quality of the output signal at the secondary side. This, in turn, results in considerable pulsations of the signal at the receiver [22]–[24], [54]. Pulsations are referred to as transient variations in the signal's amplitude followed by its return to the initial value and they have a significant impact on the efficiency [25], [26]. This thesis investigates a way to eliminate the pulsations by varying the distance between the transmitters [49]. Inadequate relative position between the transmitting coils deteriorates the quality of the received signal. In this thesis, the pulsations are estimated as the difference between the maximum and

the minimum values, namely signal variation, which is then divided by the maximum recorded amplitude to get the percentage of the signal's reduction. At the same time, however, the effect of the distance between the transmitter and the receiver as well as the impact of the rectangular coils on the pulsations are considered [27]. Therefore, one of the solutions to increase the efficiency and at the same time improve the charging process of the DWC system is to decrease the distance between the adjacent transmitting coils [21], [53].

1.2 Problem definition

The main and the most significant problem of the entire system of dynamic wireless charging of electric vehicles is its low efficiency, which is caused by pulsation of output power signal. Generally, pulsations are created due to dynamic behavior of the system, in other words, when vehicle passes transmitters and gaps between them, it faces fluctuations of output power signal in receiver side. These pulsations considerably decrease overall efficiency of the system and can damage battery. To solve this issue, it is necessary to make the output power signal more constant and stable, which consequently means increase in efficiency. So, it is important to decrease the level of pulsations and overcome the problem with efficiency by investigating different cases with shape of coils and distance between coils.

1.3 Objective

Thus, the main aim of the given thesis is to analyze the behavior of the DWC system at different types of coils and distances between coils, compare simulation outputs with the practical results retrieved from the laboratory setup.

1.4 Contribution

The personal contribution to this thesis:

- Investigation and simulation of mutual inductance on ANSYS Maxwell for different cases.
- Study on mathematical model and simulation of entire Dynamic Wireless Charging System of Electric Vehicles on Simulink.
- Investigation of behavior of magnetic flux density and its simulation on ANSYS Maxwell.
- Simulation of several cases for reduction of output power pulsations. Generally, different types of coils and different distances between coils were examined on ANSYS Maxwell.
- Experimental results were obtained from the prototype of dynamic wireless charging system and compared with simulation outputs.

1.5 Thesis outline

Chapter 2 discusses different cases of mutual and self-inductances depending on number of coils. In addition, this chapter compares the simulation and practical results of mutual inductances obtained from ANSYS Maxwell and LCR-8105G Precision LCR Meter respectively. Dynamic Wireless Charging System design, its mathematical model and behavior of magnetic flux density are discussed in Chapter 3. Experimental results of the entire system are presented in Chapter 4. Retrieved experimental results are discussed and compared with simulation outputs in Chapter 5. Finally, Chapter 6 provides conclusion of main points of the thesis and suggests future work.

Chapter 2 – Mutual Inductance Measurement Technique

Chapter 2 presents the method used to estimate self- and mutual inductances of the coils in different conditions as well as provides a comparison of the mutual inductances obtained from the simulation results and their practical measurements produced using LCR-8105G Precision LCR Meter.

In this thesis it is very important to analyze the self-inductance and mutual inductance between coils because it has significant influence on efficiency of the system and power transmission characteristics. In addition, since the system is dynamic, the mutual inductance becomes variable and it is necessary to investigate the factors affecting to the change of mutual inductance.

2.1 Determination of self- and mutual inductances

Figure 1 illustrates the winding model of the two coils (A and B) with an air-core. According to [28], the self- and mutual inductances of the coils depend only on the geometric parameters of the windings.

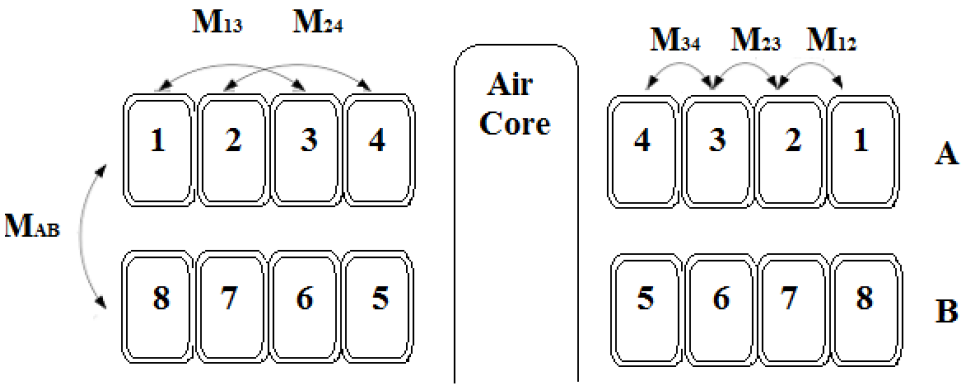

Figure 2.1.1: Winding model of two coils with an air core

The term M_{AB} in Figure 2.1.1 is the mutual inductance between the discs *A* and *B*, M_{12} is the turn to turn mutual inductance between the turns 1 and 2. Considering Figure 2.1.1, the inductance matrix of the disc *A* and mutual inductance matrix of the discs *A* and *B* are obtained as:

$$L_A = \begin{pmatrix} L_1 & M_{12} & M_{13} & M_{14} \\ M_{21} & L_2 & M_{23} & M_{24} \\ M_{31} & M_{32} & L_3 & M_{34} \\ M_{41} & M_{42} & M_{43} & L_4 \end{pmatrix}, M_{AB} = \begin{pmatrix} M_{15} & M_{16} & M_{17} & M_{18} \\ M_{25} & M_{26} & M_{27} & M_{28} \\ M_{35} & M_{36} & M_{37} & M_{38} \\ M_{45} & M_{46} & M_{47} & M_{48} \end{pmatrix} \quad (2.1.1)$$

where L_1 is the turn's inductance.

The total self-inductance of the disc A, $L_{A\text{-}disc}$ is found via the integration of all the mutual and self-inductances of each turn. Thus,

$$L_{A\text{-}disc} = L_1 + L_2 + L_3 + L_4 + 2\begin{pmatrix} M_{12} + M_{13} + M_{23} \\ + M_{14} + M_{24} + M_{34} \end{pmatrix} \quad (2.1.2)$$

$$M_{A\text{-}disc} = 2\left(M_{12} + M_{13} + M_{23} + M_{14} + M_{24} + M_{34}\right) \quad (2.1.3)$$

Equations (2.1.2), (2.1.3) can be extended for different number of turns and discs [21].

2.2 Case of one transmitter and one receiver

It is important to understand the methodology employed to estimate the mutual inductance in different systems. In order to determine its value, it is critical to estimate the self-inductance of the coils. Figure 2.2.1 demonstrates two mutually coupled coils, which are connected in series and have their self-inductances denoted as L_1 and L_2. The inductors are connected in such a way that their magnetic fields are oriented in the same direction. Hence, the voltages across the inductors can be obtained as:

$$V = V_1 + V_{M,1} + V_2 + V_{M,2} \tag{2.2.1}$$

where $V_{M,1}$ and $V_{M,2}$ are the voltages created by the mutual inductance M between the coils, while L_1 and L_2 induce the voltages V_1 and V_2, respectively. Taking into account the fact that the magnetic fields of the coils are in the same direction, all of the voltages are positive terms. In addition, $V_{M,1}$ and $V_{M,2}$ should be equal due to the identical dimensions of the coils. Applying Lenz's law, the voltage, V induced into the system becomes:

$$V = -L_1 \frac{dI}{dt} - M \frac{dI}{dt} - L_2 \frac{dI}{dt} - M \frac{dI}{dt} = -(L_1 + L_2 + 2M) \frac{dI}{dt} \tag{2.2.2}$$

According to (2.2.2), the self-inductance of the system, L is then obtained as:

$$L = L_1 + L_2 + 2M \tag{2.2.3}$$

Solving (2.2.3) in terms of *M*, would result in:

$$M = \left(L - (L_1 + L_2)\right)/2 \tag{2.2.4}$$

Also, the mutual inductance can be determined if the inductors have the magnetic fields of the opposing direction.

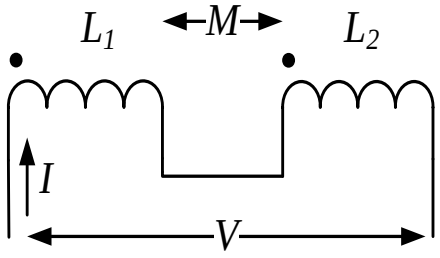

Figure 2.2.1: Series connected coils with the same magnetic field direction

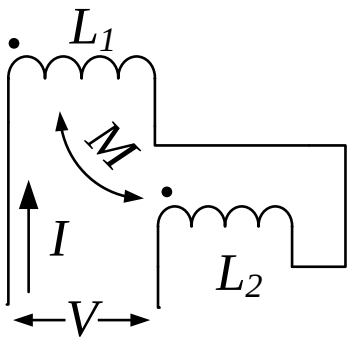

Figure 2.2.2: Series connected coils with the opposing magnetic field direction

According to Figure 2.2.2, the voltage, *V*, induced into the system can be found as:

$$V = V_1 - V_{M,1} + V_2 - V_{M,2} = \tag{2.2.5}$$
$$-L_1 \frac{dI}{dt} + M \frac{dI}{dt} - L_2 \frac{dI}{dt} + M \frac{dI}{dt} = -(L_1 + L_2 - 2M)\frac{dI}{dt}$$

From (2.2.5), the self-inductance, L of the system with the opposing magnetic fields becomes:

$$L = L_1 + L_2 - 2M \tag{2.2.6}$$

Then, the mutual inductance is obtained as:

$$M = \left((L_1 + L_2) - L\right)/2 \tag{2.2.7}$$

2.3 Case with several transmitters and one receiver

In case of DWC systems for EVs, several transmitting coils interact with the receiving one. Thus, Figure 2.3.1 depicts the case of four transmitters and one receiver. From Figure 2.3.1, it is clearly observed that there are four mutual inductances formed in such configuration, i.e. M_{15}, M_{25}, M_{35}, M_{45}.

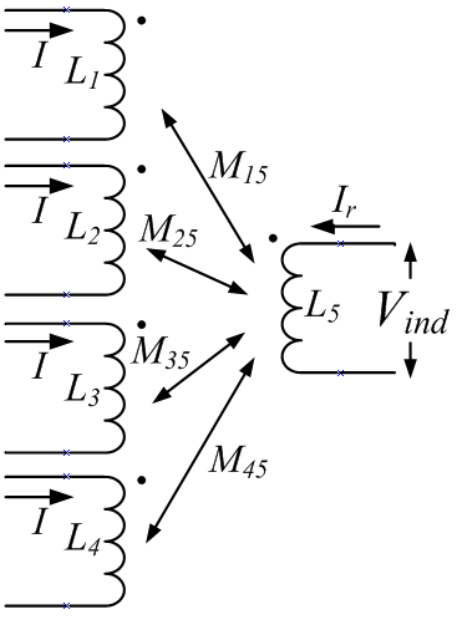

Figure 2.3.1: System with four transmitters and one receiver

Therefore, the voltage induced into the receiver, V_{ind} can be obtained as:

$$V_{ind} = -L_5 \frac{dI_r}{dt} - (M_{15} + M_{25} + M_{35} + M_{45}) \frac{dI}{dt} \quad (2.3.1)$$

As it can be noted from (2.3.1), V_{ind} is formed by the self-induced electromotive force and the mutual coupling between the transmitters and the receiver. Therefore, the total mutual inductance in the system with multiple transmitters would be determined by the summation of the individual mutual inductances between the coils [20], [21].

2.4 Simulation and experimental result of the mutual inductance estimation for one transmitter and one receiver

The dimensions provided in Table 2.4.1, are utilized in modeling, simulation and experimental analysis.

Table 2.4.1: Transmitting and receiving coils parameters

Parameter	**Transmitting and receiving coils**
Number of turns	18
Inner diameter	140 mm
Conductor diameter	4 mm
Interturn spacing	3 mm
Outer diameter	400 mm

The distance between the transmitting and the receiving coils was taken to be equal to 6 cm and the coils were excited by a 6 A current source. The circular planar coils were manufactured using copper wires with circular cross section. Their self-inductances were estimated to be 86.8 μH at the design stage. Figure 2.4.1 illustrates isometric and top views of the simulated coils.

(a) (b)

Figure 2.4.1: Simulated coils in perfect alignment: (a) isometric view, (b) top view

For the experimental results, the distance between the transmitting and the receiving coils remained equal to 6 cm, and the parameters of the fabricated coils were taken to be as presented in Table 2.4.1. Experimental self-inductances for the transmitting and the receiving coils were measured to be 93.3 μH and 90.8 μH, respectively. A possible reason for higher values in experimental results compared to the simulation output can be extra wirings and conductors, which were used to connect the circuit. The variable mutual inductance was obtained by considering different positions of the receiver with respect to the transmitters. Precisely, the former was moved, strictly parallel to the

latter, along 11 positions, which correspond to -50 cm, -40 cm, -30 cm, -20 cm, -10 cm, 0 cm, 10 cm, 20 cm, 30 cm, 40 cm, and 50 cm between the centers of the transmitter and the receiver, respectively. In other words, this means that the receiving coil moves above the transmitting coil's center for 100 cm along the *x*-axis. Table 2.4.2 and Figure 2.4.2 demonstrate the simulation and experimental results of this movement.

Table 2.4.2: Simulation and experiment results of mutual inductance for different receiver positions

Position #	Simulated Mutual inductance (μH)	Experimental Mutual inductance (μH)	Position #	Simulated Mutual inductance (μH)	Experimental Mutual inductance (μH)
1	-1.11	-1.32	7	27.9	29.7
2	-2.23	-2.69	8	6.63	6.33
3	-2.64	-3.04	9	-2.63	-3.77
4	6.62	4.75	10	-2.21	-3.18
5	27.9	28.3	11	-1.12	-2.20
6	41.1	40.4			

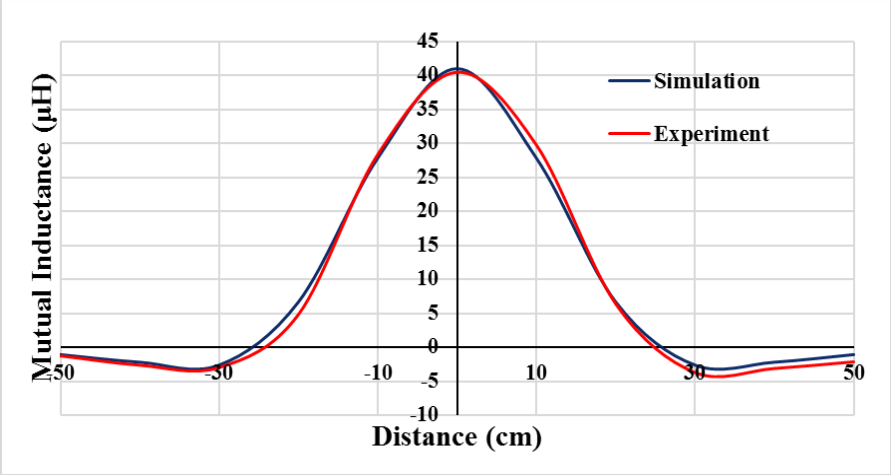

Figure 2.4.2: Comparison of experimental and simulated mutual inductances for different positions of receiving coil

According to Figure 2.4.2, it is clearly observed that the experimental and simulation results are in a desirable agreement. In both cases, as the receiving coil moves away from the perfect alignment position, the mutual inductance of the system decreases significantly.

2.5 Simulation of mutual inductance for one receiver and several transmitters

A 3D simulation for the case of one receiver and several transmitters is presented in Figure 2.5.1. It should be stated that the radius of the simulated coils was taken to be 20 cm. The mutual inductance of the system is directly related to the overall power transfer's efficiency. Thus, in order to analyze the behavior of the system's mutual inductance, the distances between the transmitters' sides were taken to be 10 cm and 0 cm. Moreover, the mutual inductance variation at 10 cm overlap was also examined. From Figure 2.5.2, it can be observed that the minimum mutual inductance between the transmitter and the receiver occurs when the former passes the gap between the latter. In addition, due to this gap the overall behavior of the system's mutual inductance (red line) demonstrates severe fluctuations.

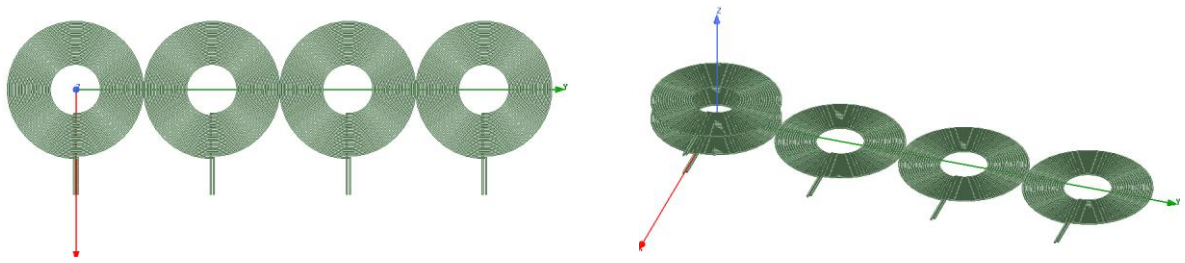

(a) (b)

Figure 2.5.1. Simulation of a multi transmitter system for 0 cm gap between them: (a) top view, (b) 3D view

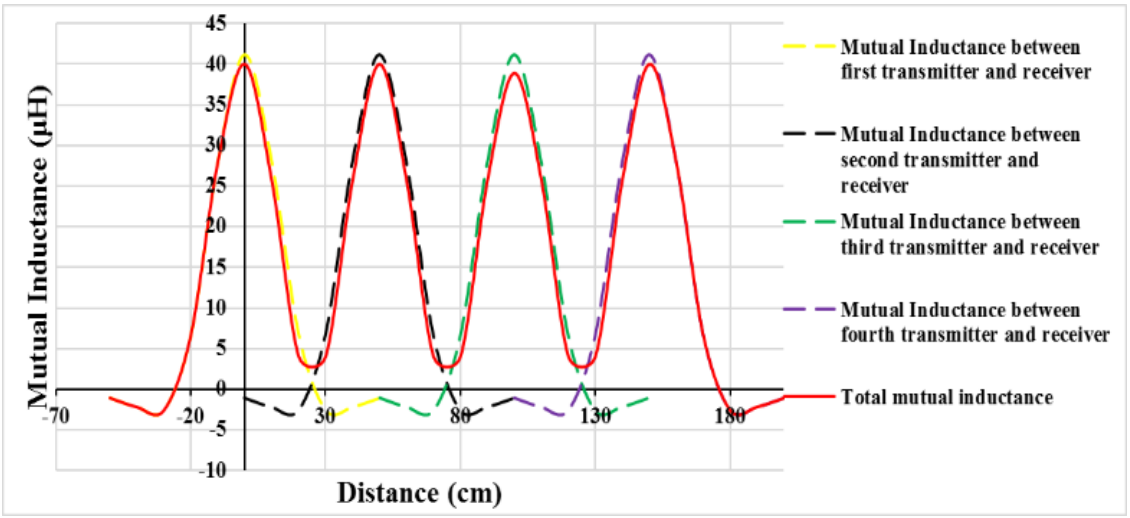

Figure 2.5.2: Mutual inductance between transmitting and receiving coils for a 10 cm gap between transmitters

If the gap between the transmitters is decreased, the mutual inductance at the times when the receiver crosses it, tends to increase and stabilize. Precisely, in case of 0 cm gap and 10 cm overlap between the transmitters depicted in Figure 2.5.3 and Figure 2.5.4, respectively, the mutual inductance of the system experiences less drastic drops as compared to the results in Figure 2.5.2.

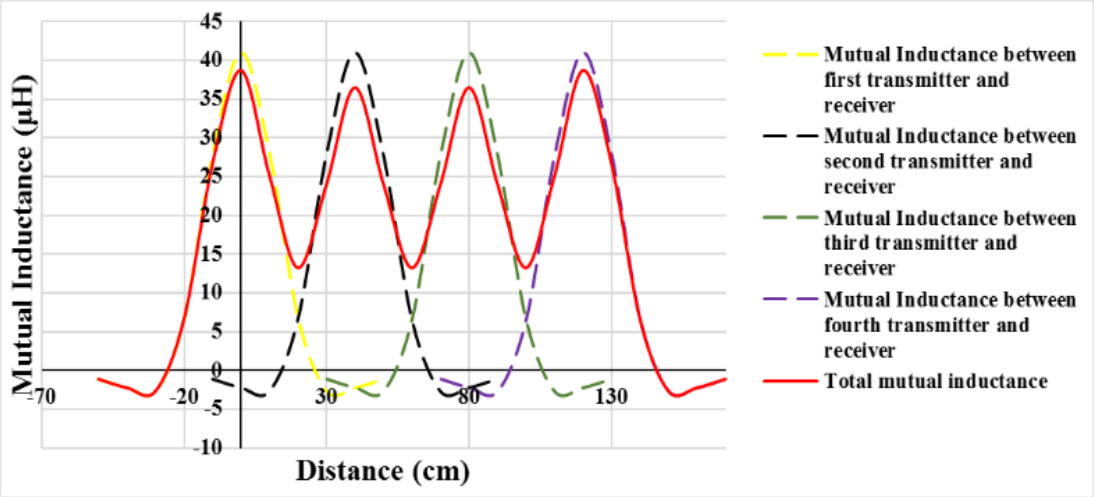

Figure 2.5.3: Mutual inductance between transmitting and receiving coils for a 0 cm gap between transmitters

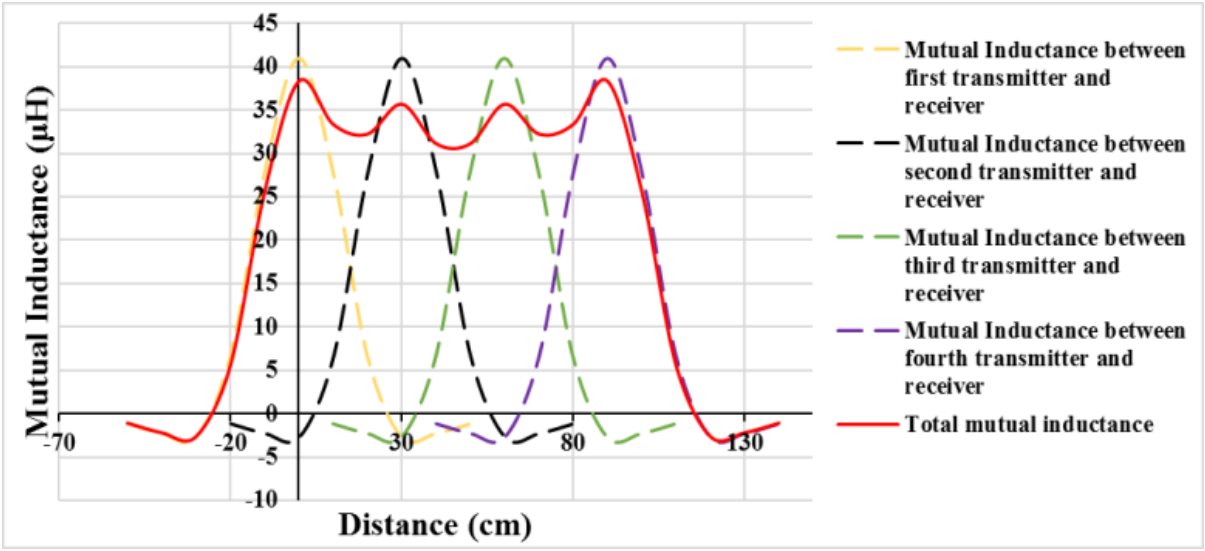

Figure 2.5.4: Mutual inductance between transmitting and receiving coils for a 10 cm overlap between transmitters

In addition, it can also be observed that the system's mutual inductance is higher at the first and the last coils. This happens due to the fact that there is no opposing magnetic flux created by the neighboring transmitting coil, since when the receiver passes the first or the last coil only one transmitter is active. The simulation has shown that the smaller the distance between the transmitters, the higher the mutual

inductance between the coils is obtained. By applying this knowledge, the problem with the power pulsations of the system can be mitigated. However, it is projected that the case when transmitting coils overlap each other may be unfeasible.

Chapter 3 – EV Dynamic Wireless Charging System Model

Chapter 3 concentrates on a DWC system's design, mathematical modeling and demonstrates the emulation results. The electromagnetic flux density, which is one of the indicators of the WPT system's safety, is also simulated and discussed in this section.

Generally, this chapter focuses on entire system of Dynamic Wireless Charging with all of the components, which is explained in detail. Furthermore, the simulation results of mutual inductance as well as output voltage and power for different cases such as: several distances between transmitter and receiver, rectangular and circular coil shapes have been shown in this chapter. The idea of simulations was to compare factors which influence the output voltage and power the most.

3.1 Description of dynamic wireless charging system's layout

The DWC system's model, illustrated in Figure 3.1.1, consists of an inverter, compensation circuits, one receiving coil, four transmitting coils and switches.

Inverter converts the input DC voltage to the AC signal. The benefit of using AC signal is higher efficiency in coupling, otherwise, for DC signal there is no voltage induced on receiver side [34], [61].

Switches are employed to minimize losses and therefore increase the efficiency by turning on and off the transmitters when it is required [38], [41].

Compensation circuit is utilized to filter undesired noises from the input signal and tune it to a resonant frequency [32], [35]. In addition, the compensation circuit decreases the reactive power in the circuit model, which significantly increases the efficiency [40].

Transmitting coils installed into the road's surface generate the magnetic field and radiate it for the receiver to pick up [39].

Receiving coil is magnetically coupled to the transmitting ones and receives the energy from them using WPT [37].

The modeled system works at 20 kHz with the 18 V DC source used as an input. Other circuit's parameters are shown in Table 3.1.1. It should be highlighted that the values for inductors L_{11}, L_{22}, L_{33}, L_{44} and capacitors C_{12}, C_{22}, C_{32} and C_{42} are selected in such a way that ensures a perfect resonant condition at 20 kHz [44], [57]. This in turn allows to achieve higher efficiency by cancelling reactance of the power electronic components. In addition, resistances such as R_1, R_2, R_3, R_4, R_{11}, R_{21}, R_{31}, R_{41}, R_{12}, R_{22}, R_{32}, R_{42} and capacitances such as C_1, C_2, C_3, C_4, C_5 are specific parameters of used wire. In other words, the values were taken after measuring wire parameters with LCR meter and implemented in simulation.

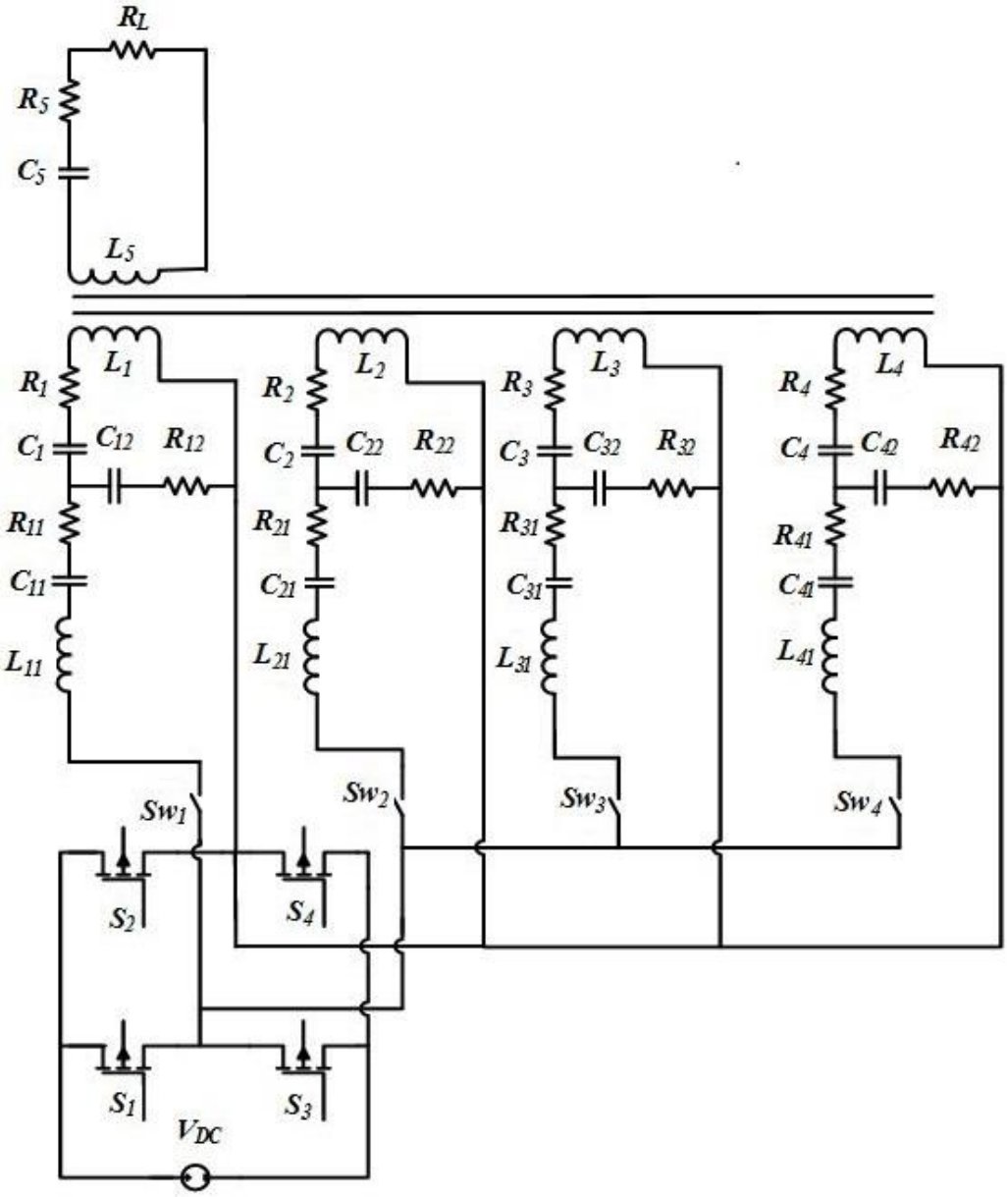

Figure 3.1.1: Overall circuit's layout of DWC System

Table 3.1.1: Circuit parameter values

Parameter	**Value**
L_1, L_2, L_3, L_4, L_5	90 μH
R_1, R_2, R_3, R_4,	250 mΩ
C_1, C_2, C_3, C_4, C_5	690 nF
L_{11}, L_{21}, L_{31}, L_{41}	13 μH
R_{12}, R_{22}, R_{32}, R_{42}	15 mΩ
C_{12}, C_{22}, C_{32}, C_{42}	6 μF
R_{11}, R_{21}, R_{31}, R_{41}	40 mΩ
R_L	15 Ω

3.2 Mathematical model

In order to model the behavior of the system, mesh current analysis was applied to the circuit illustrated in Figure 3.1.1. The following matrix describes the system in terms of impedances *Z*, currents, *I* and voltages, *U*:

$$\begin{pmatrix} Z_{11} & Z_{12} & 0 & 0 & Z_{15} & Z_{16} & 0 & 0 & 0 \\ Z_{21} & Z_{22} & Z_{23} & 0 & Z_{25} & 0 & Z_{27} & 0 & 0 \\ 0 & Z_{32} & Z_{33} & Z_{34} & Z_{35} & 0 & 0 & Z_{38} & 0 \\ 0 & 0 & Z_{43} & Z_{44} & Z_{45} & 0 & 0 & 0 & Z_{49} \\ Z_{51} & Z_{52} & Z_{53} & Z_{54} & Z_{55} & 0 & 0 & 0 & 0 \\ Z_{61} & 0 & 0 & 0 & 0 & Z_{66} & 0 & 0 & 0 \\ 0 & Z_{72} & 0 & 0 & 0 & 0 & Z_{77} & 0 & 0 \\ 0 & 0 & Z_{83} & 0 & 0 & 0 & 0 & Z_{88} & 0 \\ 0 & 0 & 0 & Z_{12} & 0 & 0 & 0 & 0 & Z_{99} \end{pmatrix} \begin{pmatrix} I_1 \\ I_2 \\ I_3 \\ I_4 \\ I_5 \\ I_{11} \\ I_{21} \\ I_{31} \\ I_{41} \end{pmatrix} = \begin{pmatrix} 0 \\ 0 \\ 0 \\ 0 \\ 0 \\ U_{11} \\ U_{21} \\ U_{31} \\ U_{41} \end{pmatrix} \quad (3.2.1)$$

where I_1, I_2, I_3, I_4 are the transmitting coils' currents, I_5 is the receiving coil's current, I_{11}, I_{21}, I_{31}, I_{41} are the resonators' input currents, and U_{11}, U_{21}, U_{31}, U_{41} are the resonators' input voltages. Equations (3.2.2-3.2.19) estimate the impedances used in (3.2.1).

$$Z_{11} = R_1 + R_{12} + jwL_1 + 1/(jwC_1) + 1/(jwC_{12}) \quad (3.2.2)$$

$$Z_{22} = R_2 + R_{22} + jwL_2 + 1/(jwC_2) + 1/(jwC_{22}) \quad (3.2.3)$$

$$Z_{33} = R_3 + R_{32} + jwL_3 + 1/(jwC_3) + 1/(jwC_{32}) \quad (3.2.4)$$

$$Z_{44} = R_4 + R_{42} + jwL_3 + 1/(jwC_4) + 1/(jwC_{42}) \quad (3.2.5)$$

$$Z_{55} = R_L + R_5 + jwL_5 + 1/(jwC_5) \quad (3.2.6)$$

$$Z_{66} = R_{11} + R_{12} + jwL_{11} + 1/(jwC_{11}) + 1/(jwC_{12}) \quad (3.2.7)$$

$$Z_{77} = R_{21} + R_{22} + jwL_{21} + 1/(jwC_{21}) + 1/(jwC_{22}) \quad (3.2.8)$$

$$Z_{88} = R_{31} + R_{32} + jwL_{31} + 1/(jwC_{31}) + 1/(jwC_{32}) \quad (3.2.9)$$

$$Z_{99} = R_{41} + R_{42} + jwL_{41} + 1/(jwC_{41}) + 1/(jwC_{42}) \quad (3.2.10)$$

$$Z_{12} = Z_{21} = jwM_{12}; \quad (3.2.11)$$

$$Z_{23} = Z_{32} = jwM_{23}; \quad (3.2.12)$$

$$Z_{34} = Z_{43} = jwM_{34} \quad (3.2.13)$$

$$Z_{15} = Z_{51} = -jwM_{15}; Z_{25} = Z_{52} = -jwM_{25}; \quad (3.2.14)$$

$$Z_{35} = Z_{53} = -jwM_{35}; Z_{45} = Z_{54} = -jwM_{45}; \quad (3.2.15)$$

$$Z_{16} = Z_{61} = -(R_{12} + 1/(jwC_{12})); \quad (3.2.16)$$

$$Z_{27} = Z_{72} = -(R_{22} + 1/(jwC_{22})); \quad (3.2.17)$$

$$Z_{38} = Z_{83} = -(R_{32} + 1/(jwC_{32})); \quad (3.2.18)$$

$$Z_{49} = Z_{94} = -(R_{42} + 1 / (jwC_{42})). \quad (3.2.19)$$

3.3 Simulation of dynamic wireless charging system

Figure 3.3.1 depicts a circuit used in the simulation. The system was built in MATLAB Simulink. As it can be observed, the mutual coupling between the coils of the system was modeled by means of controlled voltage sources. Each of the transmitting coils has a mutual coupling with the neighboring transmitter as well as with the receiver [30]. The first transmitting coil is coupled with the receiving one via a variable mutual inductance, M_{15}. At the same time, its wireless connection to the second transmitting coil is described by a mutual inductance term, M_{12}. In case of the second transmitter, apart from being coupled with the first transmitting coil and the receiver via the mutual inductances M_{25} and M_{21}, respectively, it is also connected to the third transmitter via a mutual inductance term, M_{23}. The system was simulated at 20kH with 18 V DC source as input. Also, for compensation circuit was taken LCC circuitry due to its higher efficiency and better power characteristics. Generally, values for inductors L_{11}, L_{22}, L_{33}, L_{44} and capacitors C_{12}, C_{22}, C_{32}, C_{42} are chosen to resonate at 20kHz. Selecting proper values is important because it helps to cut out unnecessary frequencies from inverter and increases the fundamental frequency. Additionally, by choosing proper values for components the reactive power flowing in the system can be significantly decreased. In addition, there are

some specific resistance and capacitance values of wire which were measured using LCR meter and mentioned in Section 3.1. All of the component values are shown on Table 3.1.1.

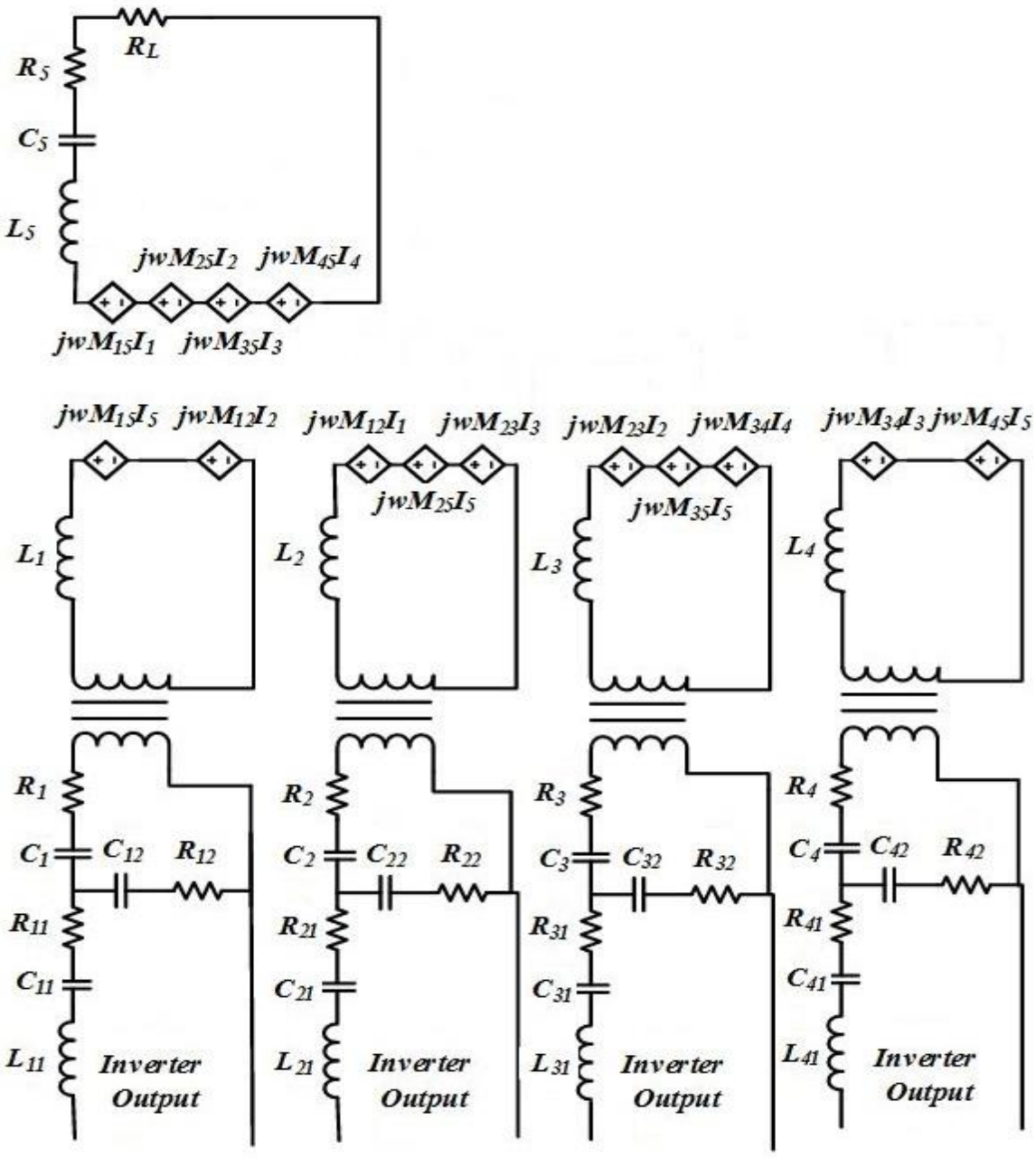

Figure 3.3.1: Mutual coupling of the system simulated in Simulink

3.4 Simulation results of dynamic wireless charging system

In this simulation, three cases for adjacent transmitting coils' distances were considered. The transmitters were situated with 10 cm and 0 cm gaps as well as placed with a 10 cm overlap between each other. From Figures 3.4.1-3.4.3 the behavior of the receiver's voltage can be clearly observed. One can conclude that the recorded pulsations can be decreased by reducing the distances between the transmitting coils.

In fact, since the receiver's load is represented by a resistance, the power received at the secondary side of the system is directly proportional to the voltage. This, in turn, means, that such plunges in the voltage's amplitude at the receiver, will lead to significant power amplitude's variations as well as to losses. Consequently, the overall efficiency of the system can potentially be increased by means of compensating the discussed pulsations.

In order to assess the level of the output signal's pulsations at different distances between the transmitters, the method proposed in Section I is employed. It implies that the difference between the maximum and the minimum points retrieved from the Figures 3.4.1-3.4.3 is divided by the peak value. Thus, from Figure 3.4.1 (b) representing the case of 10 cm distance between the transmitters, the pulsation percentage is equal to (70-23)/70=0.672, which corresponds to 67.2%; from Figure

3.4.2 (b) representing the case of 0 cm gap the percentage is given as (65-29)/65=0.554 which accounts for 55.4%; from Figure 3.4.3 (b) representing the case of 10 cm overlap, the pulsation percentage is calculated as (72-58)/72=0.194 which amounts in 19.4%. Hence, the method of placing transmitting coils close to each other considerably decreases the pulsations and makes the output voltage and power signals smoother. Additionally, the system was simulated with one and four transmitting coils to investigate the behavior of the magnetic flux density.

In fact, the magnetic flux has a direct influence onto the excitation of the receiving coil and the power transfer. Therefore, it is important to consider the performance of the system in terms of magnetic flux density. From Figure 3.4.4, it can be seen that the solid red lines at the bottom of the graph represent the transmitting coils' positions. The receiving coil moves over them, and its magnetic flux density is recorded. Generally, the behavior of the magnetic flux density is similar to the one of the mutual inductances in Figures 2.4.2 and 2.5.2.

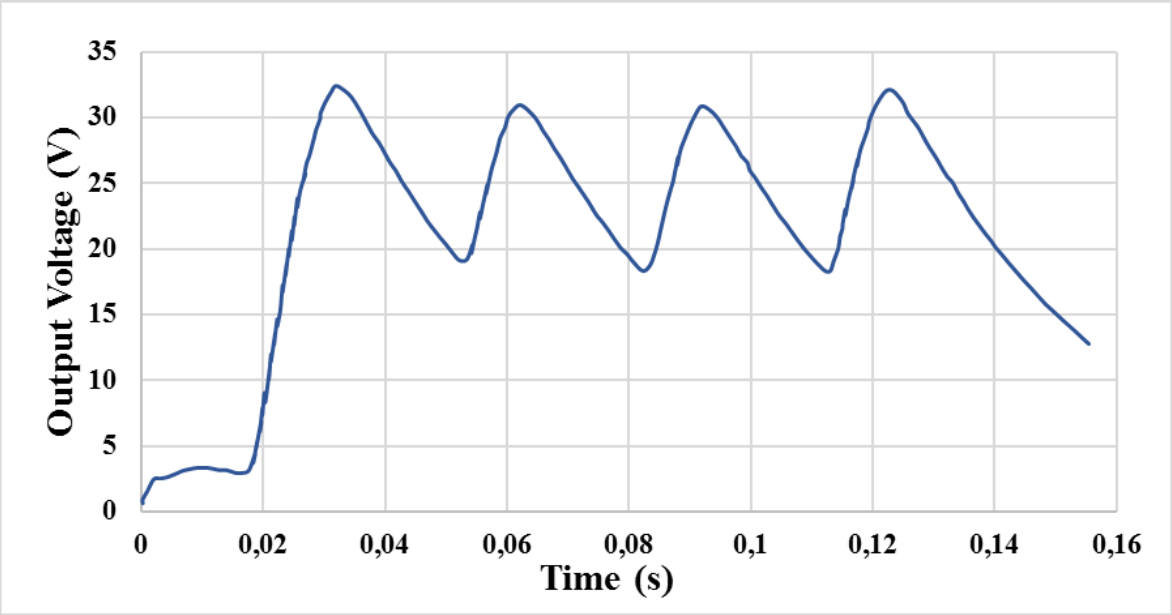

(a)

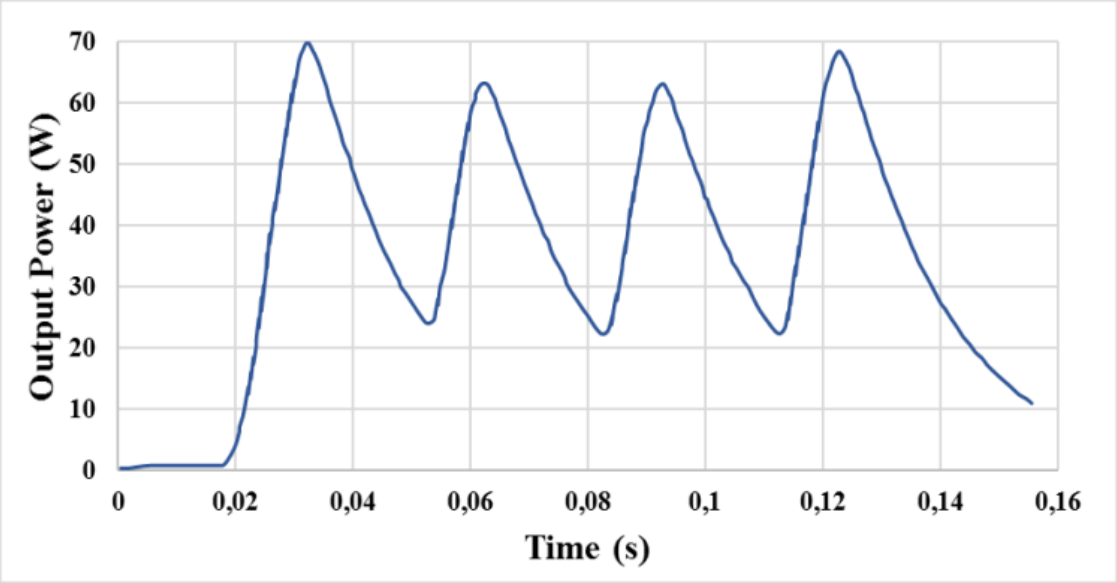

(b)

Figure 3.4.1: Output Voltage (a) and Output Power (b) of the system with 10 cm gap between transmitting coils

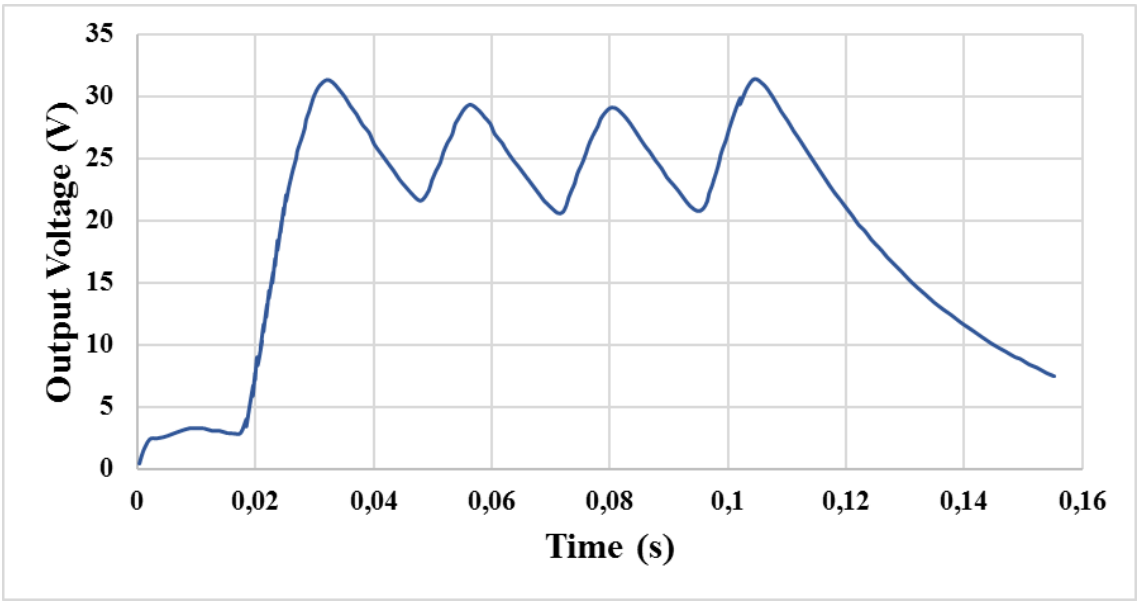

(a)

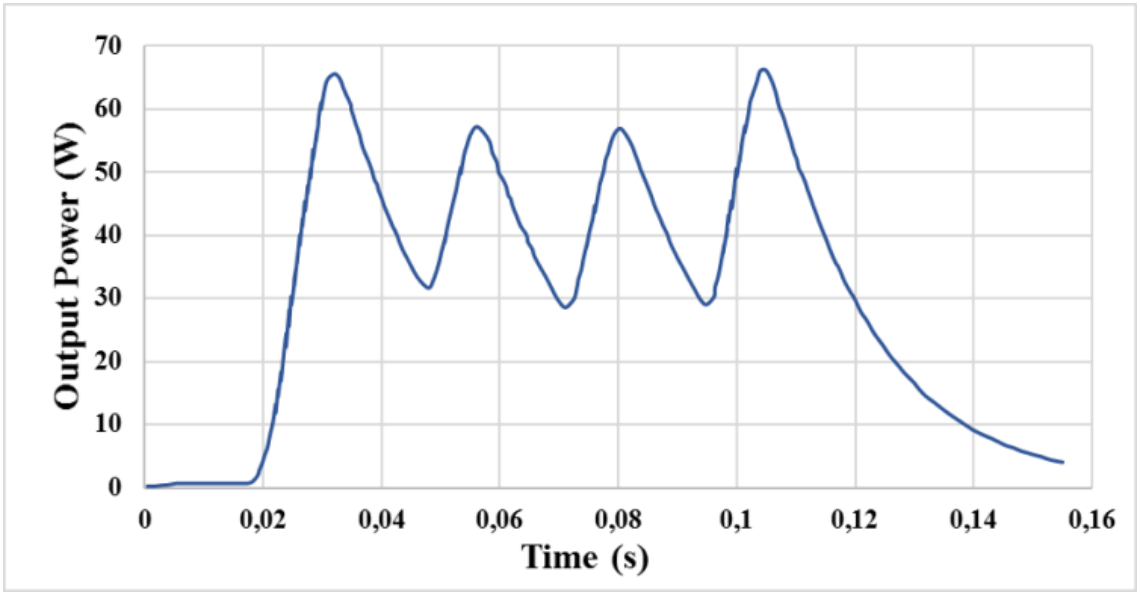

(b)

Figure 3.4.2: Output Voltage (a) and Output Power (b) of the system with 0 cm gap between transmitting coils

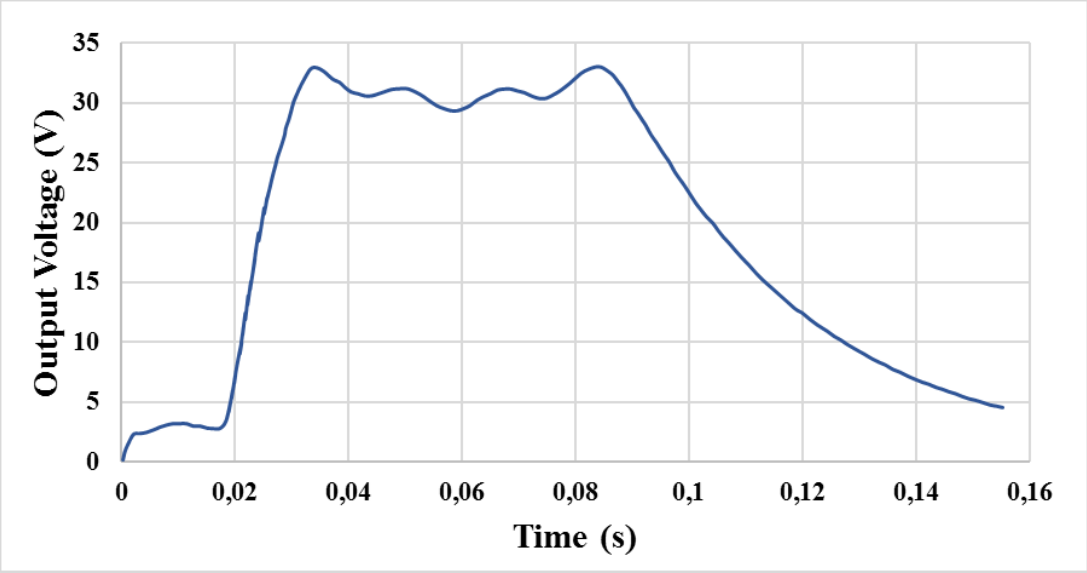

(a)

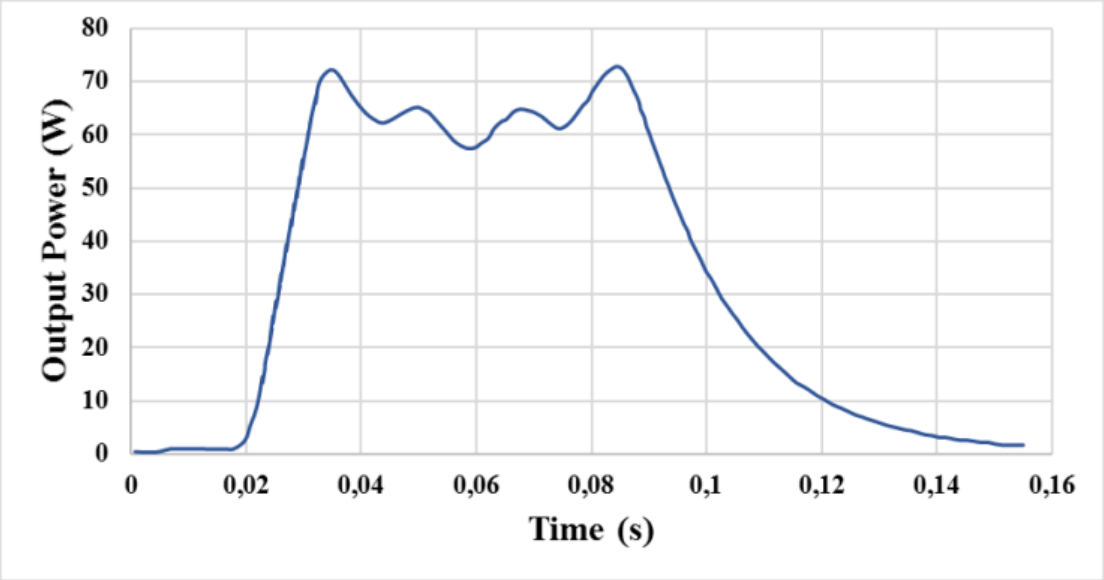

(b)

Figure 3.4.3: Output Voltage (a) and Output Power (b) of the system with 10 cm overlap between transmitting coils

The only difference which can be highlighted is the small oscillations at the peak of each pulsation. In Figure 3.4.4 (a), the small decrease in magnetic flux happened due to the nature of the flux lines. Precisely, they are created by the excited coil and tend to curve to the right or left, depending on the direction of the current. Thus, at the point of perfect alignment between any transmitter and the receiver the magnetic flux density reduces due to the geometry of the flux lines. One of the possible reasons for the drop at the first pulsation and increase at the last one in Figure 3.4.4 (b) can be switching between the coils. It implies that when only one coil is activated, it has higher magnetic flux density because there is no opposing flux created by another coil. This pattern does not occur at the second and third pulsations due to the fact that while passing that region, at least two coils remain activated at the same time. Thus, the magnetic flux density's magnitude at the second and the third pulsations in Figure 3.4.4 (b) is less than at the first and the last ones.

The system was also modelled in a simulator to identify a safe distance from the coils at which the magnetic flux will be tolerable to a human body. The coils were placed in a box with the parameters of 50 cm, 170 cm and 20 cm in *x*-, *y*-, and *z*-axis respectively. According to the International Commission on Non-Ionizing Radiation Protection (ICNIRP) [22], the allowable magnetic flux for the frequency range 3 kHz-10 MHz is 27 μT at the distances of maximum 20 cm.

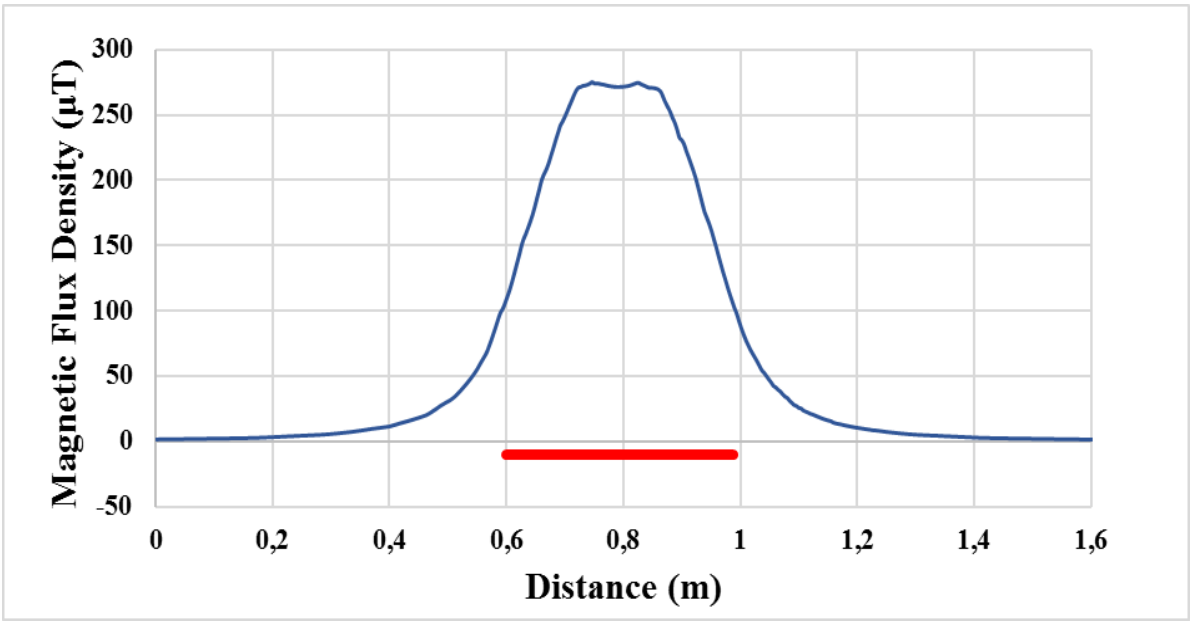

(a)

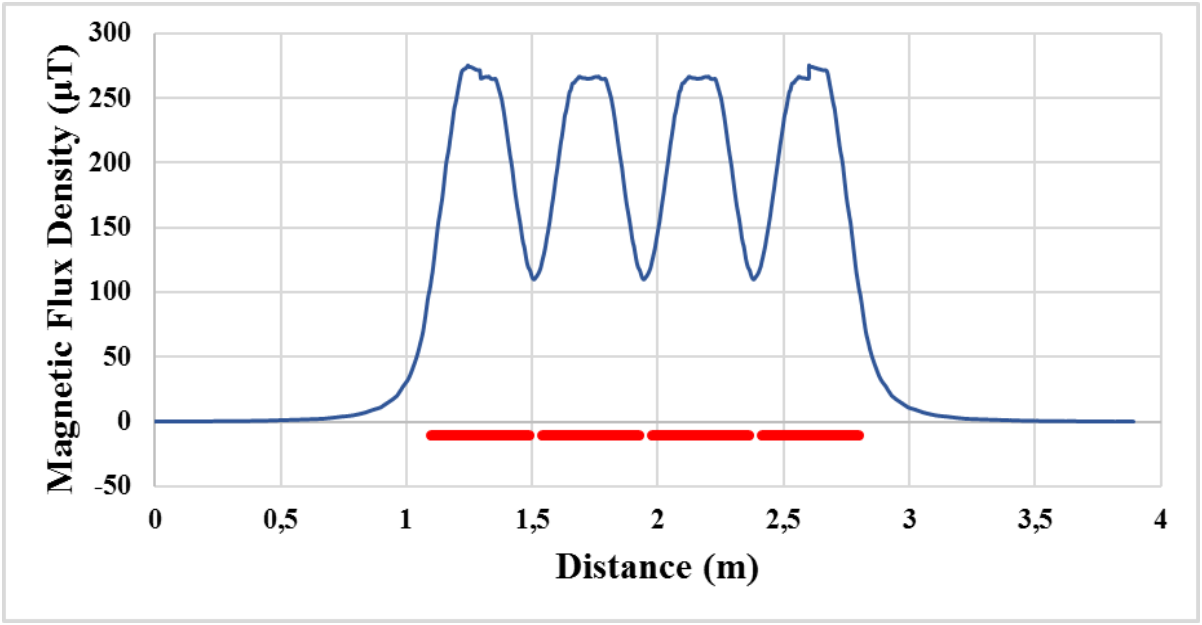

(b)

Figure 3.4.4: Magnetic flux density behavior of one transmitter (a) and four transmitters (b)

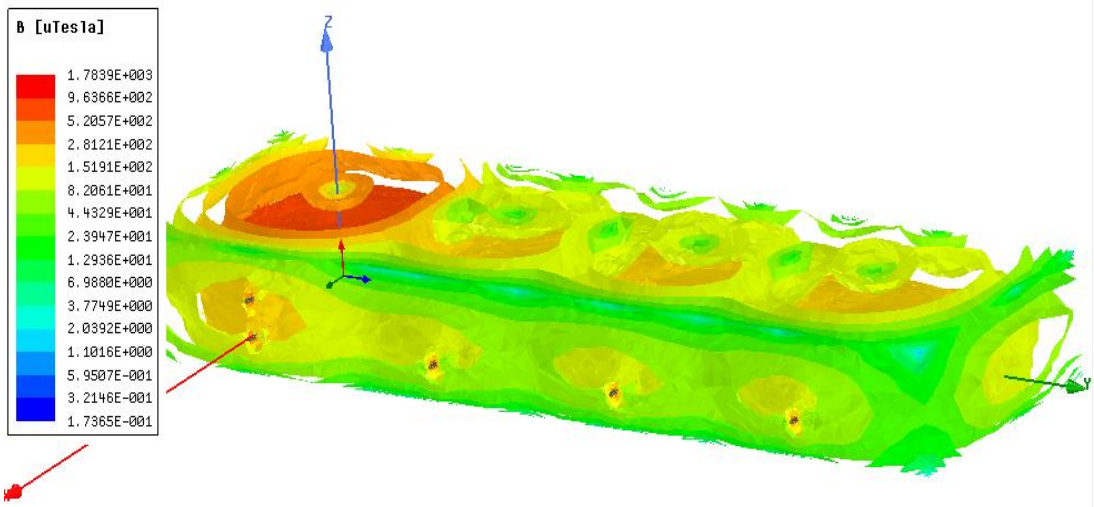

Figure 3.4.5: Transmitting and receiving coils' magnetic flux visualization and assessment

In other words, if the magnetic flux exceeds 27 μT at the distances greater than 20 cm from its source, it is considered harmful for a human health. From Figure 3.4.5, it is clearly seen that the value of the magnetic flux produced by the given DWC system for EV is less than 27 μT even at 20 cm distance from the excited coils.

Alternatively, there are two other methods to decrease the output power pulsations, namely changing the distance between the transmitting and the receiving coils as well as selecting a different coils' shape.

As it was mentioned in Chapter II, the distance between the transmitter and the receiver was chosen to be 6 cm. In addition, the system has been simulated at the distances of 1 cm and 11 cm in order to assess the feasibility of the first approach.

According to Figure 3.4.6, as it was expected the high level of mutual inductance was reached when the coils were positioned close to each other.

Moreover, Figures 3.4.7-3.4.8 show that positioning transmitting and receiving coils closer increases the output voltage and power. In order to estimate the output power pulsation's level mathematically, the difference between the maximum and the minimum points on the pulsations' plot are divided by the amplitude. Thus, from Figure 3.4.8, it can be observed that at the distance of 11 cm the percentage of pulsation is equal to (48-14)/48=0.708, which corresponds to 70.8%. Moreover, at the distance of 6 cm the percentage can be calculated as (70-23)/70=0.671 which results in 67.1%. Finally, for the distance of 1 cm the percentage is estimated as (120-41)/120=0.658, which amounts in 65.8%. Thus, one can conclude that the percentage of the pulsations reduces as the transmitting and the receiving coils become closer. However, the improvement is not as significant as it was expected. In fact, the pulsations reduce by 5%, due to the 10 cm reduction of the distance between the receiver and the transmitter. In practical terms this means decreasing the clearance of the EV, which will complicate their utilization by the end users. Precisely, the vehicle with a 1 cm clearance will be very problematic to employ at the regular roads.

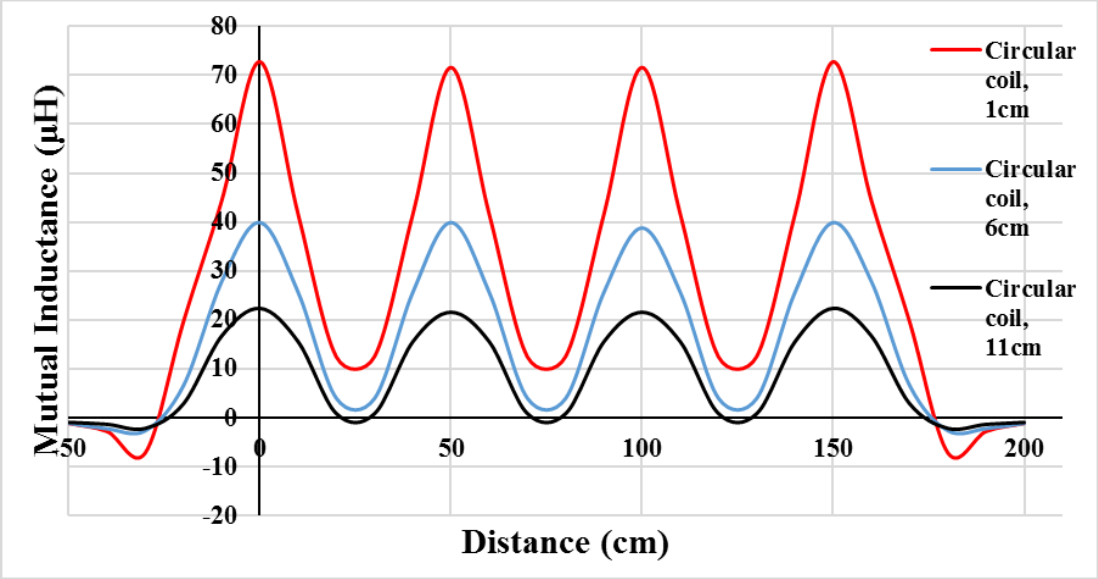

Figure 3.4.6: Mutual Inductance for different distances between the transmitter and the receiver

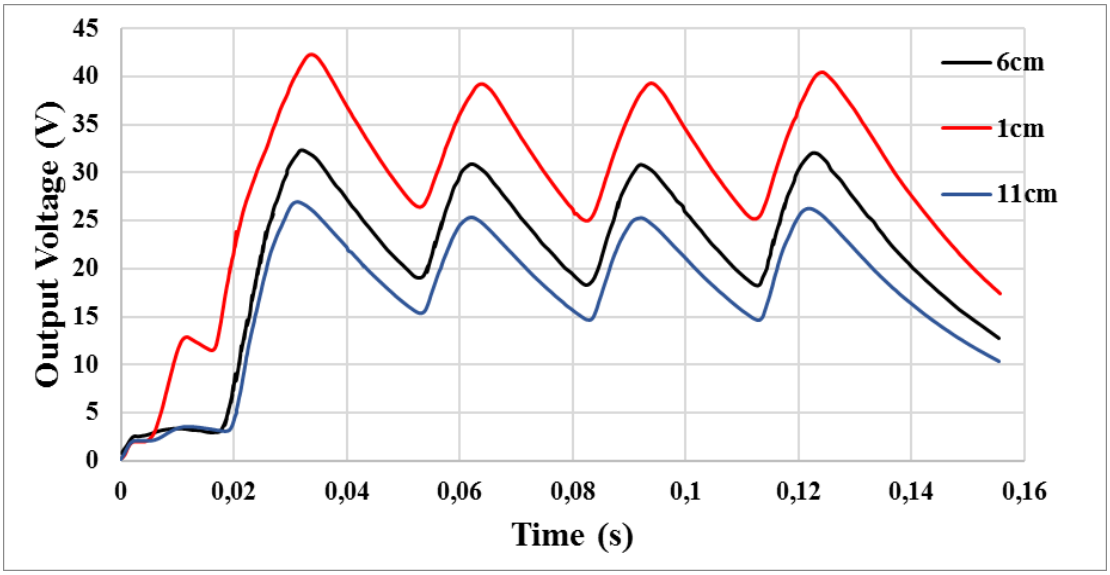

Figure 3.4.7: Output Voltage for different distances between the transmitter and the receiver

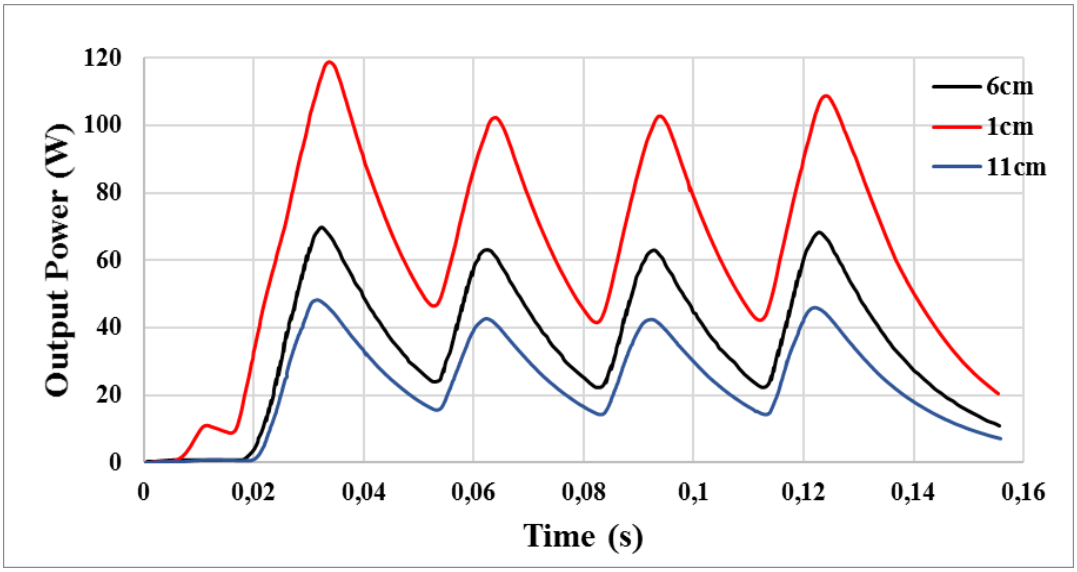

Figure 3.4.8: Output Power for different distances between the transmitter and the receiver

The second method aiming to reduce the pulsations at the receiver side implies replacing the circular shaped coils employed in the given system with the rectangular ones. According to Figure 3.4.9, the mutual inductance of the rectangular coils is less in terms of the maximum achieved magnitude compared to the circular ones. However, the pulsations are notably reduced for the rectangular coils. Figures 3.4.10-3.4.11 illustrate the output voltage and power, respectively. So, it can be said that the output voltage and power of rectangular coils are less in magnitude compared to circular coils. In terms of pulsations, the method to estimate the pulsations' percentage is also applied in this case in order to quantify the difference in the coils' performance. Hence, from Figure 3.4.11 for the circular coils the output power pulsations' percentage is calculated as (70-23)/70=0.671, which corresponds

to 67.1%. On the other hand, for the rectangular coils, it can be estimated as (37-19)/37=0.487, which amounts in 48.7%.

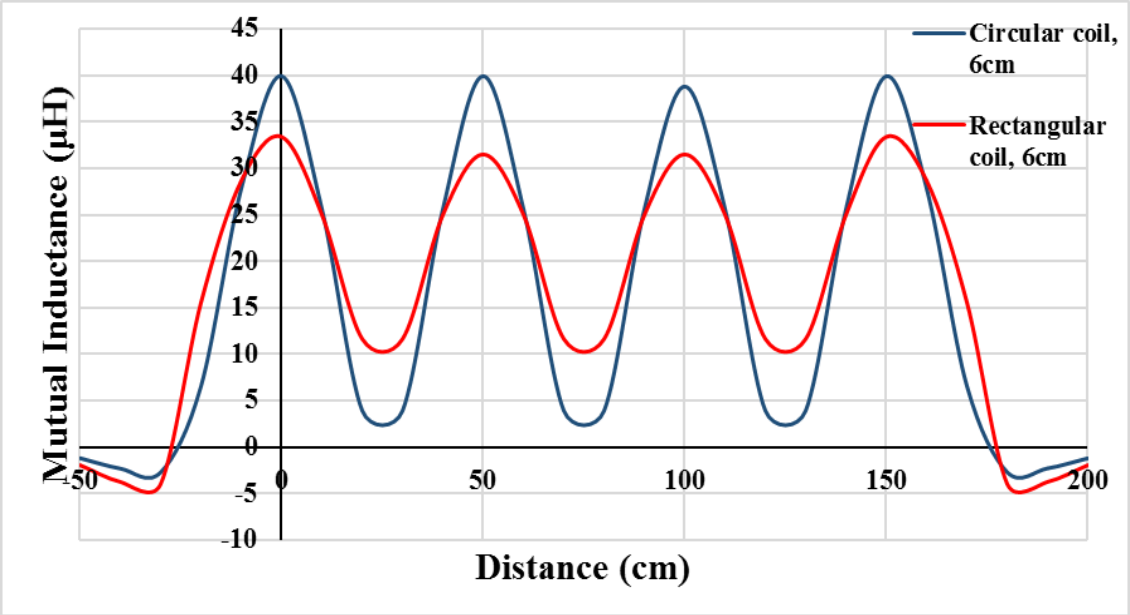

Figure 3.4.9: Mutual Inductance for different coils

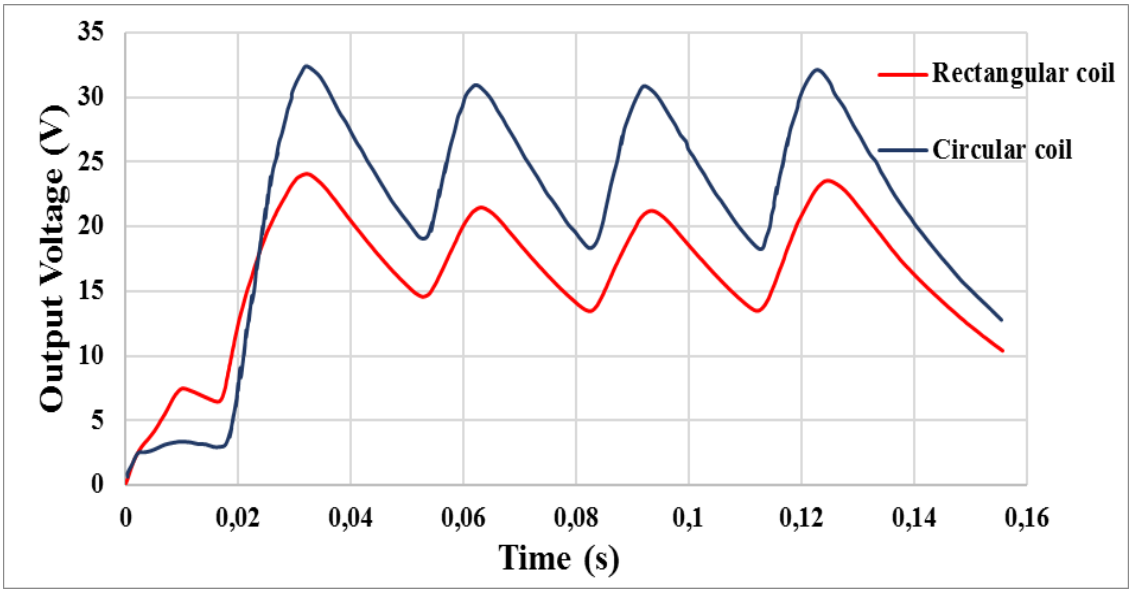

Figure 3.4.10: Output Voltage for different coils' shapes

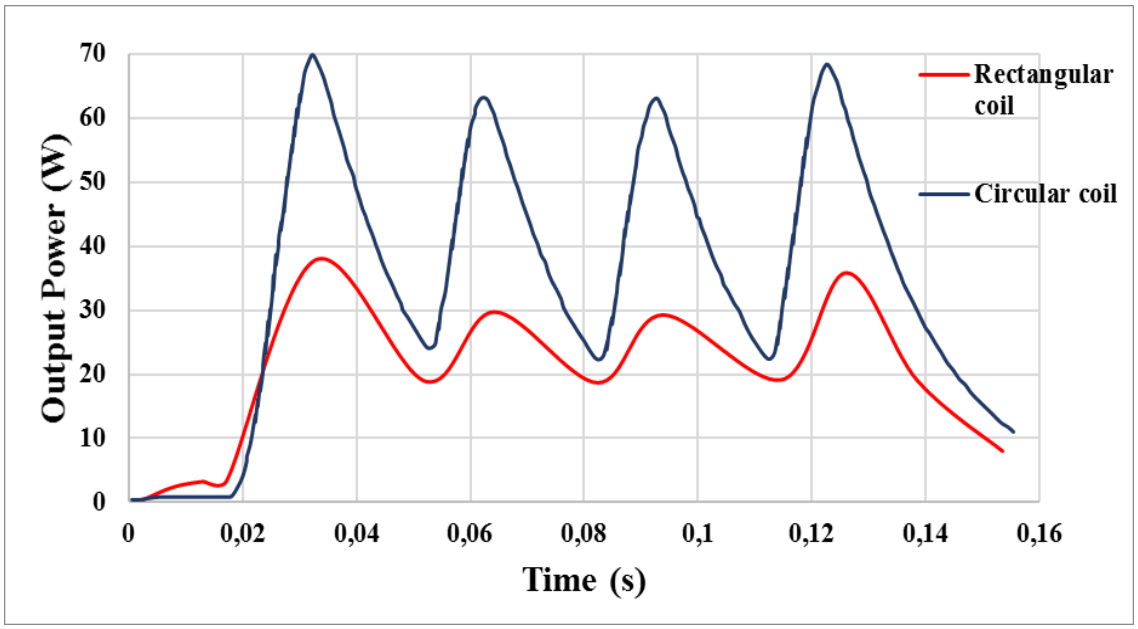

Figure 3.4.11: Output Power for different coils' shapes

Thus, one can easily conclude that the pulsations' percentage is less for the rectangular coils. However, despite of the fact that they show better performance in terms of pulsation, the transmitted power for them is significantly less compared to the circular coils. Precisely, the maximum power values are 37 W and 70 W, respectively. It means that the rectangular coils provide more stable output power than the circular ones, but the level of that power is considerably less.

Chapter 4 – Experiment Results

The experimental setup along with the practical results obtained is presented in this chapter.

The DWC system presented in this thesis was fabricated with all the components and in accordance with the parameters as well as dimensions presented in Chapter 3.

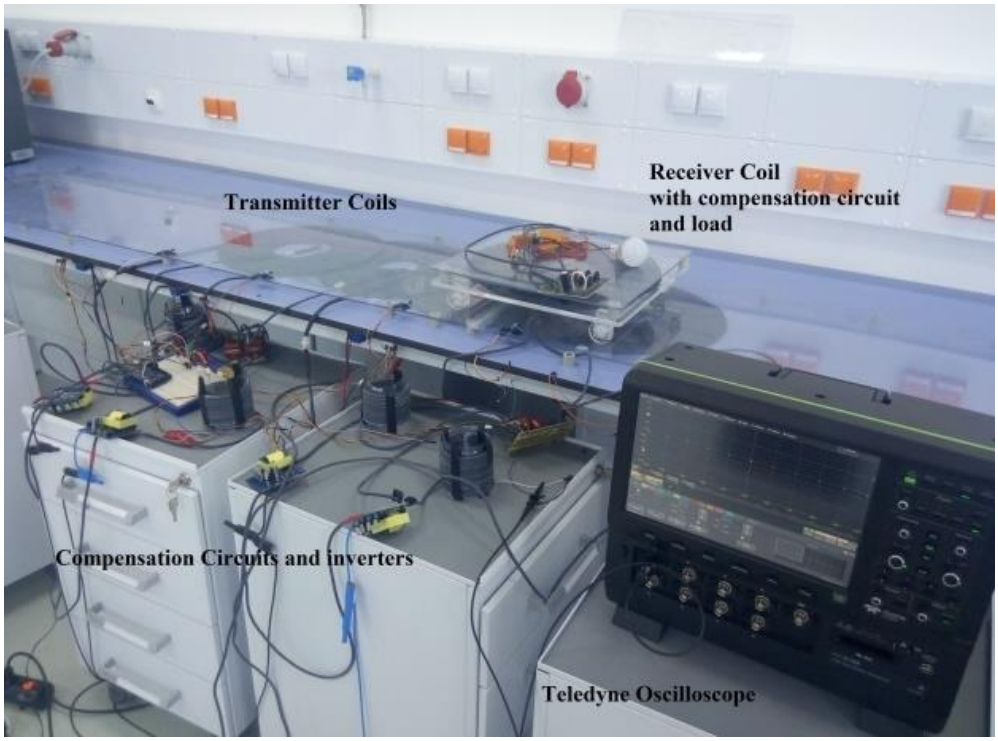

Figure 4.1: Experimental Setup of DWC EV

There are four identical transmitting coils and one receiving coil, which is located on a portable vehicle made of Plexiglas. The practical setup equipped with high definition Teledyne oscilloscope is illustrated in Figure 4.1. Figures 4.2-4.4 illustrate

the output voltage and output power which were obtained by experimental setup in laboratory conditions.

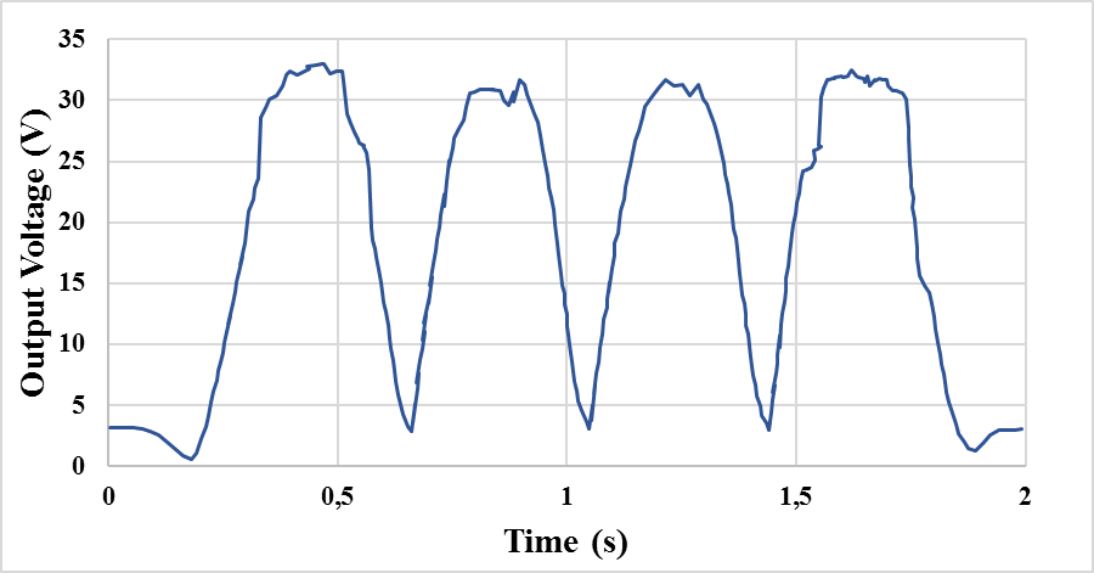

(a)

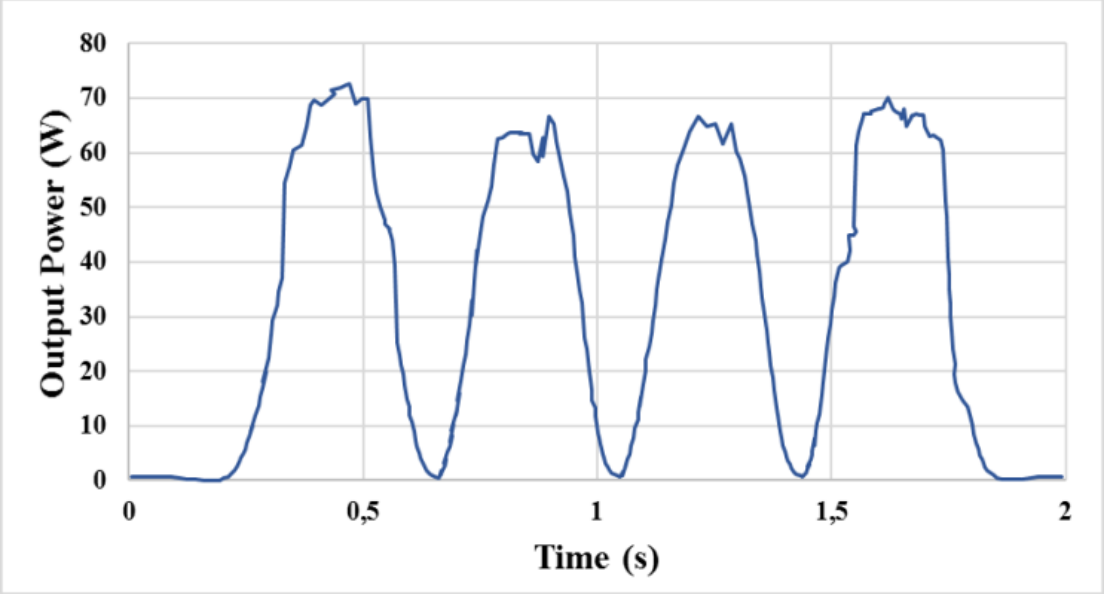

(b)

Figure 4.2: Output Voltage (a) and Output Power (b) of the system with 10 cm gap between the transmitting coils

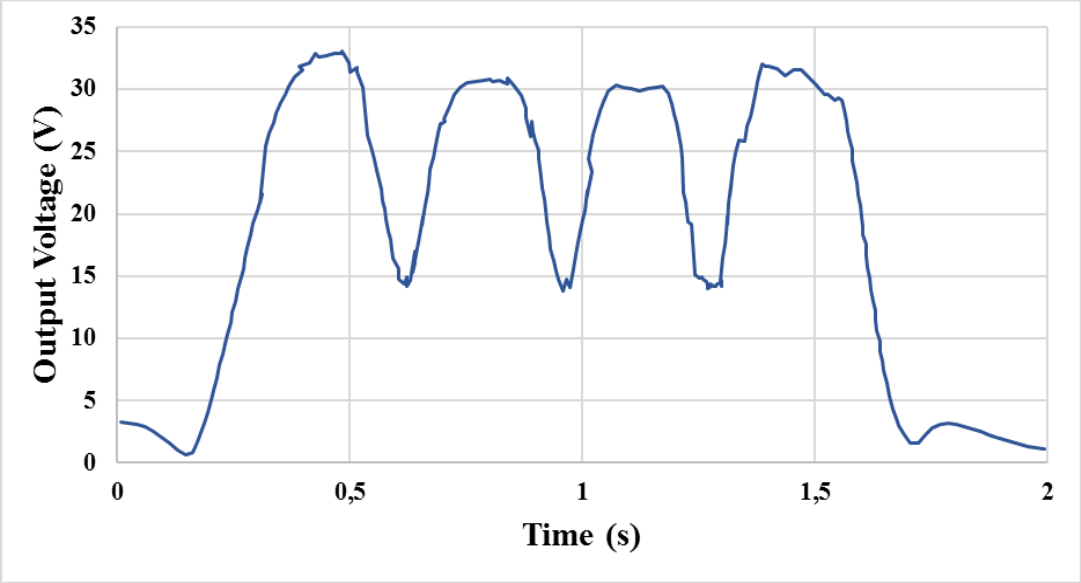

(a)

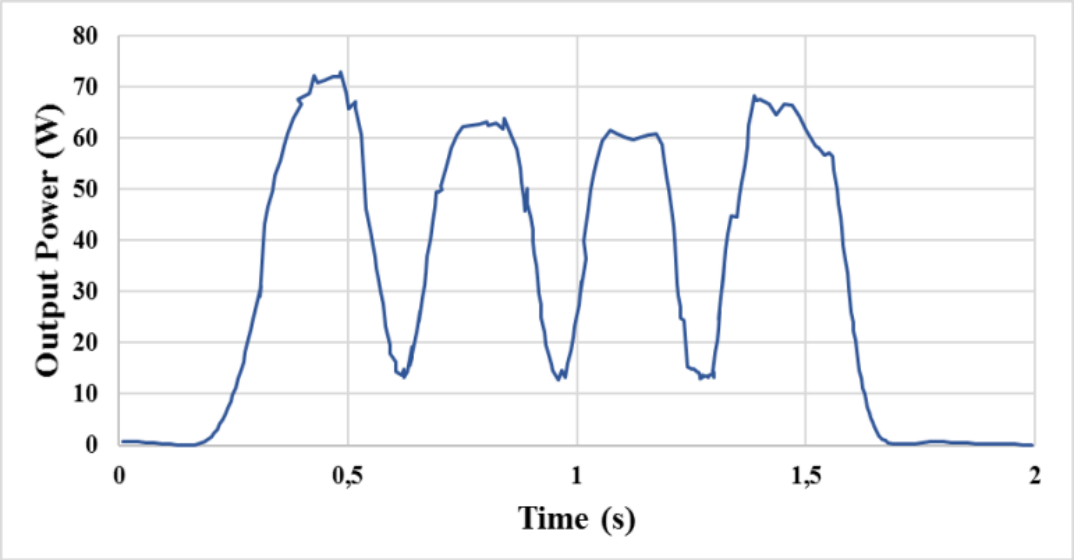

(b)

Figure 4.3: Output Voltage (a) and Output Power (b) of the system with 0 cm gap between transmitting coils

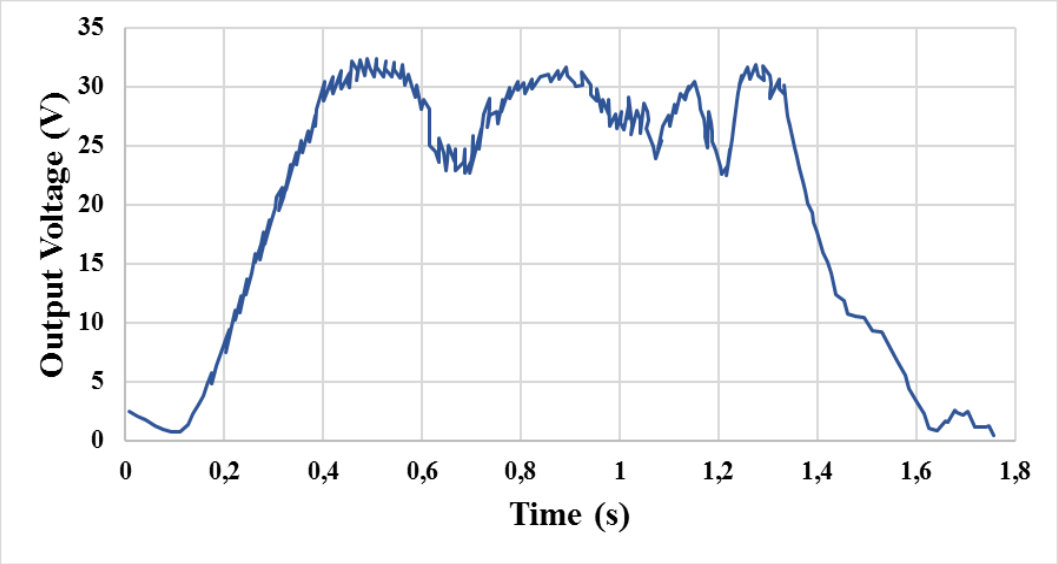

(a)

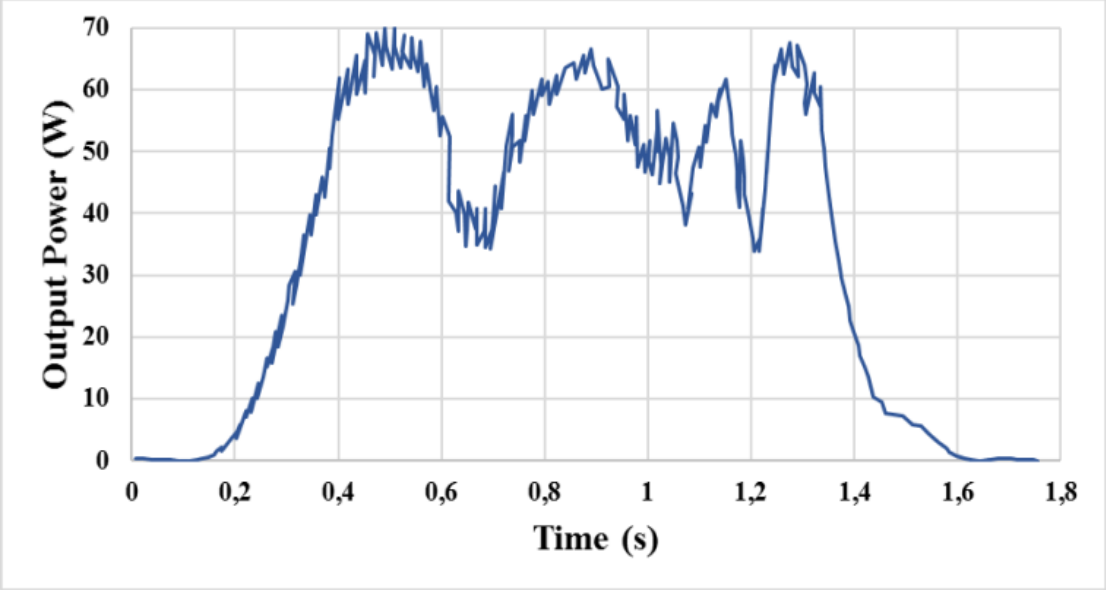

(b)

Figure 4.4: Output Voltage (a) and Output Power (b) of the system with 10 cm overlap between transmitting coils

Chapter 5 – Discussion on Practical Results

The simulated and experimental results are discussed in Chapter 5. Mainly, this chapter discusses the level of pulsation in each of the results and compares it with simulation outputs.

In this section of the thesis the simulation and experimental results of the system, namely the output voltage and power, depicted in Figures 3.4.1-3.4.3 and Figures 4.2-4.4, respectively, for different distances between the transmitters are compared. As it was mentioned in Chapter 3 the load is purely resistive meaning that the current is directly proportional to the voltage, therefore the results for the output current were neglected and only the measurements of the voltage were collected. According to Figures 3.4.1-3.4.3 and Figures 4.2-4.4, the pulsation reduction occurs with the decrease in the gap between the transmitting coils, as it was expected. Moreover, it should be highlighted that the behavior of the voltage is similar to the one demonstrated by the mutual inductance in Figures 2.5.2-2.5.4.

In addition, considering the behavior of the voltage, the maximum value was achieved when the transmitting and the receiving coils were in perfect alignment with one another. Furthermore, the range of the voltage and the power values in

simulation was the same as in the practical measurements, which means that the results are in desirable agreement.

From Figure 4.2 (b) a 10 cm gap between the transmitting coils has shown (72-0)/72=1, which is 100% of the pulsations' percentage. This, in turn, means that, it reduced from its maximum to 0W. According to Figure 4.3 (b), the power pulsations' percentage for the case of 0 cm distance is calculated as (72-14)/72=0.806 and corresponds to 80.6% pulsations. In case of the 10 cm overlap between the transmitters, from Figure 4.4. (b) one can calculate the pulsations' percentage as (70-35)/70=0.5 which amounts in 50%. These estimations prove that as the distance between the transmitting coils decrease, the pulsations' percentage of output power reduces, and the system becomes more stable.

Despite of the fact that the theoretical and practical results are similar, some minor discrepancies can be observed. The most visible one implies that the experimental results are not as smooth as compared to the simulation outcomes. In other words, there are some additional harmonics in the retrieved waveform. Since the experiment was performed in the laboratory conditions, speed of the portable vehicle was not uniform. Therefore, one of the possible reasons for such oscillations can be a deviating speed of the vehicle. In addition, from the experimental results, the voltage is rapidly decreasing and the experimental values of the voltage at the points when the receiver passes the gaps between the transmitters are less compared to the

simulation results. This can be explained by the internal resistance of the capacitors, which influences the time constant and result in fast decline.

Moreover, the behavior of the voltage waveform is the same as the one produced by the mutual inductance. Figures 2.5.2-2.5.4, demonstrate that the outer coils' mutual inductances are higher than those of the inner ones. The possible reason for this observation can be an opposing magnetic flux created once the adjacent transmitting coils are turned on. This consequently leads to the reduction of the mutual inductance and its relation to the voltage discussed in Chapter 2.

It can be also stated that the power output graphs for the simulation and the practical results demonstrate a desirable agreement except for the regions where the gaps occur. In case of these regions, the experimental results start to sharply decrease, whereas the simulations' output declines less steeply. A possible technical reason for this can be internal resistances of the components, which were not considered in the simulation.

Thus, the pulsations at the receiver side of the DWC system for EV can be improved by means of reducing the distance between the transmitting coils. However, bringing them closer together may not become economically attractive as the number of the coils per one meter of the road will become high at the same time increasing the material intensity of the system and its price. Hence, a combination

of adjusting the distance between the transmitters and changing the shape of the coils may be recommended. It should be also highlighted, however, that the rectangular coils have a worse performance in DWC applications as compared to the circular coils, which are very effective in terms of mutual coupling.

Chapter 6 – Conclusion and Future work

6.1 Conclusion

The main aim of this thesis is to analyze and discuss the effect of the distance between the adjacent circular transmitting coils, their shape and the distance between the transmitting and the receiving coils on the output power pulsations in Dynamic Wireless Charging system for Electric Vehicles. These pulsations are undesirable due to their destructive effect on the total system's efficiency. In this thesis, an estimation of the mutual inductance for different cases, such as one transmitter and one receiver as well as four transmitters and one receiver, rectangular and circular coils were discussed. Furthermore, the mutual inductances for different distances between the transmitters were investigated. In both cases experimental and simulation results were obtained and they revealed a decent agreement. In addition, an analytical model of the dynamic wireless charging was discussed. The voltage and the power values for different distances between the transmitting coils were retrieved. Moreover, an experimental setup was created and explained in detail. It was also practically and mathematically proven that the output power and voltage pulsations decline when the distance between the transmitters decrease. It is worth noting that the mutual inductance between the coils plays a significant role in mitigating the problem with output power pulsations. In other words, by decreasing the mutual inductance's

fluctuations, the power pulsations can be improved. Despite of the fact that experimental and simulation's results were in reasonable agreement, the voltage and power waveforms in experimental results experienced significant oscillations. This thesis demonstrated that the reduction of the gap between the transmitting coils can significantly decrease the pulsations of the voltage and improve the power waveforms. However, bringing the transmitting coils closer together may not be feasible. Therefore, alternative solutions such as rectangular coils and different distance between the transmitting and the receiving coils were suggested and investigated. As a result of the experiments, it was recommended to employ a combination of different techniques to improve efficiency, such as utilizing rectangular coils and adjusting distances between the transmitters. Moreover, this thesis discussed the effect of the magnetic flux of the simulated coils on a human body and it was shown that the magnetic flux of the proposed dynamic wireless charging system is in the permitted range.

6.2 Future work

The future work on the topic include developing a more comprehensive circuit of the dynamic wireless charging system which will incorporate more efficient rectifiers and other types of compensation circuits. In addition, different types of cores for the coils can be considered to improve the efficiency of the system. Furthermore, the system should be tested with battery to monitor the behavior of the energy storage

system. Moreover, combination of supercapacitor with battery will significantly improve charging speed of the electric vehicle.

Chapter 7 - Bibliography/References

[1] A. Rakhymbay, A. Khamitov, M. Bagheri, B. Alimkhanuly, M. Lu, and T. Phung, "Precise Analysis on Mutual Inductance Variation in Dynamic Wireless Charging of Electric Vehicle," *Energies*, vol. 11, no. 3, p. 624, 2018.

[2] I. S. Suh and J. Kim, "Electric vehicle on-road dynamic charging system with wireless power transfer technology," *Proc. 2013 IEEE Int. Electr. Mach. Drives Conf. IEMDC 2013*, pp. 234–240, 2013.

[3] G. Buja, M. Bertoluzzo, and H. K. Dashora, "Lumped Track Layout Design for Dynamic Wireless Charging of Electric Vehicles," *IEEE Trans. Ind. Electron.*, vol. 63, no. 10, pp. 6631–6640, 2016.

[4] S. Y. Choi, B. W. Gu, S. Y. Jeong, and C. T. Rim, "Advances in wireless power transfer systems for roadway-powered electric vehicles," *IEEE J. Emerg. Sel. Top. Power Electron.*, vol. 3, no. 1, pp. 18–36, 2015.

[5] S. Y. Choi, B. W. Gu, S. Y. Jeong, and C. T. Rim, "Advances in Wireless Power Transfer Systems for Roadway-powered Electric Vehicles," *IEEE J. Emerg. Sel. Top. Power Electron.*, vol. PP, no. 99, pp. 1–1, 2014.

[6] D. M. Vilathgamuwa and J. P. K. Sampath, "Wireless Power Transfer (WPT) for Electric Vehicles (EVs)—Present and Future Trends", *Plug In Electric Vehicles in Smart Grids*, *Springer*, pp. 33–61, 2015, DOI:https://doi.org/10.1007/978-981-287-299-9

[7] T. Yasuda, "Proposal of the Passive Type Dynamic Wireless Power Transfer System for EVs," *2017 19th European Conference on Power Electronics and Applications (EPE'17 ECCE Europe)*, DOI**:** 10.23919/EPE17ECCEEurope.2017.8099077

[8] V. Kindl, M. Zavrel, P. Drabek and T.Kavalir, "High Efficiency and Power Tracking Method for Wireless Charging System Based on Phase-Shift Control," *Energies*, vol. 11, p. 2065, 2018.

[9] A. Ahmad, Z. A. Khan, and M. S. Alam, "A Review of the Electric Vehicle Charging Techniques , Standards , Progression and Evolution of EV Technologies in Germany A Review of the Electric Vehicle Charging Techniques , Standards , Progression and," *Smart Sci.*, vol. 477, no. January, pp. 1–18, 2018.

[10] Y. J. Kim, D. Ha, W. J. Chappell, and P. P. Irazoqui, "Selective Wireless Power Transfer for Smart Power Distribution in a Miniature-Sized Multiple-Receiver System," *IEEE Trans. Ind. Electron.*, vol. 63, no. 3, pp. 1853–1862, 2016.

[11] C. Wang, C. Zhu, K. Song, G. Wei, S. Dong, and R. G. Lu, “Primary-side control method in two-transmitter inductive wireless power transfer systems for dynamic wireless charging applications,” *2017 IEEE PELS Work. Emerg. Technol. Wirel. Power Transf. WoW 2017*, 2017.

[12] R. Tavakoli and Z. Pantic, “Analysis, Design and Demonstration of a 25-kW Dynamic Wireless Charging System for Roadway Electric Vehicles,” *IEEE J. Emerg. Sel. Top. Power Electron.*, vol. 6777, no. c, pp. 1–16, 2017.

[13] Q. Zhu, L. Wang, Y. Guo, C. Liao, and F. Li, “Applying LCC Compensation Network to Dynamic Wireless EV Charging System,” *IEEE Trans. Ind. Electron.*, vol. 63, no. 10, pp. 6557–6567, 2016.

[14] K. Song, C. Zhu, K. E. Koh, D. Kobayashi, and T. Imura, “Modeling and design of dynamic wireless power transfer system for EV applications,” *Annu. Conf. IEEE Ind. Electron. Soc.*, pp. 005229–005234, 2015.

[15] A. Zaheer, M. Neath, H. Z. Z. Beh, and G. A. Covic, “A Dynamic EV Charging System for Slow Moving Traffic Applications,” *IEEE Trans. Transp. Electrif.*, vol. 3, no. 2, pp. 354–369, 2017.

[16] J. Shin *et al.*, “Design and implementation of shaped magnetic-resonance-based wireless power transfer system for roadway-powered moving electric vehicles,” *IEEE Trans. Ind. Electron.*, vol. 61, no. 3, pp. 1179–1192, 2014.

[17] M. Kavitha, P. B. Bobba, and D. Prasad, “A comparative analysis on WPT system using various power transfer methodologies and core configurations,” *India Int. Conf. Power Electron. IICPE*, vol. 2016–Novem, 2017.

[18] K. A. U. Menon, A. Gungi, and B. Hariharan, “Efficient Wireless Power Transfer Using Underground Relay Coils,” *Comput. Commun. Netw. Technol. (ICCCNT), 2014 Int. Conf.*, 2014.

[19] X. Lu, P. Wang, D. Niyato, D. I. Kim, and Z. Han, “Wireless Charging Technologies: Fundamentals, Standards, and Network Applications,” *IEEE Commun. Surv. Tutorials*, vol. 18, no. 2, pp. 1413–1452, 2016.

[20] H. K. Dashora, G. Buja, M. Bertoluzzo, and V. Lopresto, “Analysis and design of DD coupler for dynamic wireless charging of electric vehicles,” *J. Electromagn. Waves Appl.*, vol. 5071, no. September, pp. 1–20, 2017.

[21] J. M. Miller *et al.*, “Demonstrating Dynamic Wireless Chrging of an Electric Vehicle,” *IEEE Power Electronics Magazine*, , vol. 1, no. 1,pp. 12-24, 17 March, 2014, DOI: 10.1109/MPEL.2014.2300978.

[22] S. Bala, “Minimizing Power Pulsations Seen by a Dc Source Feeding Unbalanced Single-phase Ac Distribution Circuits through Voltage Source Converters,” *2010 IEEE International Conference on Sustainable Energy Technologies (ICSET)*, December 2010, DOI: 10.1109/ICSET.2010.5684936.

[23] K. Throngnumchai, A. Hanamura, Y. Naruse, and K. Takeda, “Design and evaluation of a wireless power transfer system with road embedded transmitter coils for dynamic charging of electric vehicles,” *World Electr. Veh. J.*, vol. 6, no. 4, pp. 848–857, 2013.

[24] S. Zhou and C. C. Mi, “Multi-Paralleled LCC Reactive Power Compensation Networks and Their Tuning Method for Electric Vehicle Dynamic Wireless Charging,” vol. 63, no. 10, pp. 6546–6556, 2016.

[25] A. Molina and J. Gonzalez, *Pulse Voltammetry in Physical Electrochemistry and Electroanalysis*. Springer International Publishing, vol. 1, no 87, 2016, DOI: 10.1007/978-3-319-21251-7

[26] Z. Qiang, H. Yun-Xiao, N. Tian-lin, and X. Chen-Yang, “Analysis and Control of Dynamic Wireless Charging Output Power for Electric Vehicle,” *2017 10th Int. Conf. Intell. Comput. Technol. Autom.*, pp. 349–354, 2017, DOI: 10.1109/TIE.2017.2723867.

[27] Z. Luo, “Analysis of Square and Circular Planar Spiral Coils in Wireless Power Transfer System for Electric Vehicles,” *IEEE Transactions on Industrial Electronics*, vol. 65, no. 1, pp. 331–341, 2018.

[28] M. Bagheri, S. Nezhivenko, B. T. Phung, and T. Blackburn, “Air Core Transformer Winding Disk Deformation: A Precise Study on Mutual Inductance Variation and Its Influence on Frequency Response Spectrum,” *IEEE Access*, vol. 6, no. 7476, pp. 7476–7488, 2017.

[29] F.W.Grover, Inductance Calculations, *Courier Corporation*, Mineola, New York, USA: Dover Publications, 2009, ISBN: 0486318354.

[30] F. Lu, S. Member, H. Zhang, and S. Member, “Output Power Pulsation for Electric Vehicles,” *IEEE Transactions on Industrial Electronics.*, vol. 63, no. 10, pp. 6580–6590, 2016, DOI: 10.1109/TIE.2016.2563380.

[31] E. To, and M. Fields, “Guidelines for limiting exposure to time-varying electric and magnetic fields (1 Hz TO 100 kHz),” *Health Phys.*, vol. 99, no. 6, pp. 818–836, 2010, DOI:10.1097/HP.0b013e3181f06c86

[32] W. Zhang and C. C. Mi, “Compensation topologies of high-power wireless power transfer systems,” *IEEE Transaction on. Vehicular Technology*, vol. 65, no. 6, pp. 4768–4778, 2016, DOI: 10.1109/TVT.2015.2454292

[33] D. Patil, M. Mcdonough, J. Miller, B. Fahimi, and P. T. Balsara, “Wireless Power Transfer

for Vehicular Applications: Overview and Challenges," *IEEE Trans. Transp. Electrif.*, vol. 7782, no. c, pp. 1–1, 2017.

[34] K. Hata, T. Imura, and Y. Hori, "Maximum Efficiency Control of Wireless Power Transfer Systems with Half Active Rectifier Based on Primary Current Measurement," *2017 IEEE 3rd International Future Energy Electronics Conference and ECCE Asia (IFEEC 2017 - ECCE Asia) pp.* 1–6, 2017.

[35] Z. Pantic, S. Bai, and S. M. Lukic, "ZCS LCC -Compensated Resonant Inverter for Inductive-Power-Transfer Application," *IEEE Trans. Ind. Electron.*, vol. 58, no. 8, pp. 3500–3510, 2011.

[36] S. Jeong, M. S. Lee, K. Cho, and Y. J. Jang, "System Model and Simulation for Optimal Parameter Design of Dynamic Wireless Charging EV s," *2016 IEEE Transp. Electrif. Conf. Expo*, no. June, pp. 82–89, 2016.

[37] K. W. E. Cheng, "An Investigation of Coils Used in Dynamic Wireless Charging for Electric Vehicles," *7th International Conference on Power Electronics Systems and Applications - Smart Mobility, Power Transfer & Security (PESA)* no. February, 2018.

[38] S. Wang *et al.*, "Modeling and control methods of dynamic wireless power transfer system," *2017 IEEE Transp. Electrif. Conf. Expo, Asia-Pacific, ITEC Asia-Pacific 2017*, pp. 1–4, 2017.

[39] H.-D. Lang, A. Ludwig, and C. D. Sarris, "Convex Optimization of Wireless Power Transfer Systems With Multiple Transmitters," *IEEE Trans. Antennas Propag.*, vol. 62, no. 9, pp. 4623–4636, 2014.

[40] G. D. F. Lima and R. B. Godoy, "Modeling and prototype of a dynamic wireless charging system using LSPS compensation topology," *IEEE Transactions on Industry Applications*, pp.1-1, 2018.

[41] A. Yoshida, E. Nishiyama, and I. Toyoda, "Selective Wireless Power Transfer Using Two Transmission Coils Sandwiching Reception Coils," *2015 Int. Symp. Antennas Propag.*, pp. 1–3, 2015.

[42] B. H. Choi, B. C. Park, and J. H. Lee, "Near-Field Beamforming Loop Array for Selective Wireless Power Transfer," *IEEE Microw. Wirel. Components Lett.*, vol. 25, no. 11, pp. 748–750, 2015.

[43] J. Park and S. Nam, "Analysis of wireless power transfer characteristics for multiple receivers by time sharing technique," *Journal of the Korean Institute of Electromagnetic and Science,*vol 11(3), pp. 183–185, 2011.

[44] M. R. V. Moghadam and R. Zhang, "Multiuser Wireless Power Transfer via Magnetic Resonant Coupling: Performance Analysis, Charging Control, and Power Region

Characterization," vol. 2, no. 1, pp. 72–83, 2015.

[45] G. Yang, M. R. V. Moghadam, and R. Zhang, "Magnetic beamforming for wireless power transfer," *ICASSP, IEEE Int. Conf. Acoust. Speech Signal Process. - Proc.*, vol. 2016–May, pp. 3936–3940, 2016.

[46] M. R. Vedady Moghadam and R. Zhang, "Node Placement and Distributed Magnetic Beamforming Optimization for Wireless Power Transfer," *IEEE Trans. Signal Inf. Process. over Networks*, vol. 1, pp. 1–1, 2017.

[47] G. Yang, M. R. V. Moghadam, and R. Zhang, "Magnetic MIMO Signal Processing and Optimization for Wireless Power Transfer," vol. 65, no. 11, pp. 2860–2874, 2017.

[48] F. Rahmani, M. R. Barzegaran, and M. Ieee, "Dynamic Wireless Power Charging of Electric Vehicles Using Optimal Placement of Transmitters," vol. 61, no. 3, p. 5090, 2016.

[49] A. Ong, P. K. S. Jayathurathnage, J. H. Cheong, and W. L. Goh, "Transmitter Pulsation Control for Dynamic Wireless Power Transfer Systems," *IEEE Trans. Transp. Electrif.*, vol. 3, no. 2, pp. 418–426, 2017.

[50] O. C. Onar, J. M. Miller, S. L. Campbell, C. Coomer, C. P. White, and L. E. Seiber, "A novel wireless power transfer for in-motion EV/PHEV charging," *Conf. Proc. - IEEE Appl. Power Electron. Conf. Expo. - APEC*, pp. 3073–3080, 2013.

[51] S. Li and C. C. Mi, "Wireless Power Transfer for Electric Vehicle Applications," *IEEE J. Emerg. Sel. Top. Power Electron.*, vol. 3, no. 1, pp. 4–17, 2015.

[52] K. A. Kalwar, M. Aamir, and S. Mekhilef, "Inductively coupled power transfer (ICPT) for electric vehicle charging - A review," *Renew. Sustain. Energy Rev.*, vol. 47, pp. 462–475, 2015.

[53] Q. Yang, Y. Li, J. Zhu, X. Zhang, Z. Yuan and Y. Li. "Coil design and efficiency analysis for dynamic wireless charging system for electric vehicles". *IEEE Trans. Magn.* 52.7 (2016), pp. 1–4

[54] Z. Hu, C. Rong, S. Wang, J. Chen and M. Liu. "Optimisation design for series–series dynamic WPT system maintaining stable transfer power". *IET Power Electron.* 10.9 (2017), pp. 987–995.

[55] S. Q.Li and C.C.Mi. "Wireless power transfer for electric vehicle applications". *IEEE J. Emerg. Sel. Topics Power Electron.* 3.1 (2015), pp. 4–17.

[56] Nam Pyo Suh Seungyoung Ahn and Dong-Ho Cho. "Charging up the road". *IEEE Spectrum* 50.4 (2013), pp. 44–50. doi: 10.1109/MSPEC.2013.6481699.

[57] S. Liu, M. Liu and C. Ma. “A High-Efficiency/Output Power and Low-Noise Megahertz Wireless Power Transfer System Over a Wide Range of Mutual Inductance”. *IEEE Transactions on Microwave Theory and Techniques* 65.11 (2017), pp. 4317–4325.

[58] L. Y. Wang, K. Strunz, K. Young and C. Wang. “Electric vehicle battery technologies”. *Springer,Electric Vehicle Integration into Modern Power Networks* 14 (2013), pp. 45–56

[59]M. Ruhul Amin and R. Roy. “Design and simulation of wireless stationary charging system for hybrid electric vehicle using inductive power pad in parking garage”. *The 8th International Conference on Software, Knowledge, Information Management and Applications (SKIMA 2014)*. Dhaka, Bangladesh, 2014.

[60] X. Jingjing and W. Guanghai. “Battery Management System of Electric Vehicle Based on CAN”. *International Conference on Intelligent Transportation, Big Data and Smart City*. 2015.

[61] V. Cirimele, S. G. Rosu, M. Khalilian and P. Guglielmi. “A dynamic wireless charging system for electric vehicles based on dc/ac converters with sic mosfet-igbt switches and resonant gate-drive”. *42nd Annual Conference of the IEEE Industrial Electronics Society*. 2016.

[62] N. D. Mazharov, S. M. Hristov, A. Dichev, and I. S. Zhelezarov, “Some Problems of Dynamic Contactless Charging of Electric Vehicles,” *Acta Polytech. Hungarica*, vol. 14, no. 4, pp. 7–26, 2017.

Appendices

Appendix A

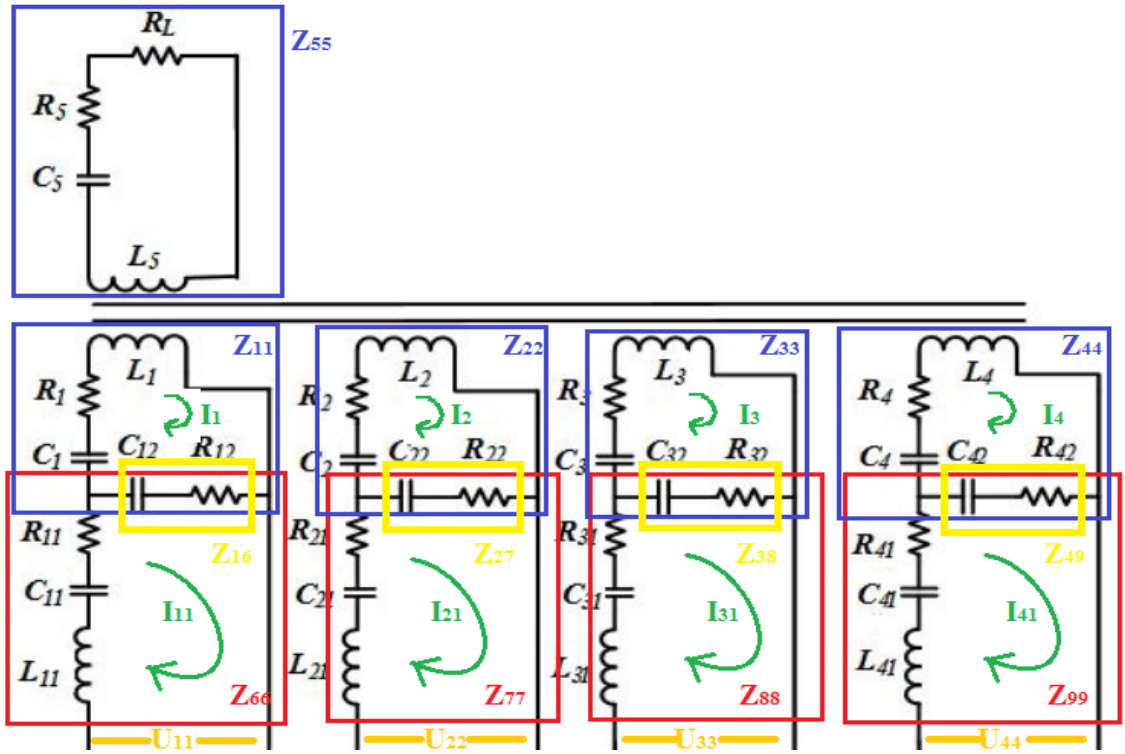

Figure A.1: Detailed schematic of DWC System

$$Z_{11}I_1 + Z_{12}I_2 + Z_{15}I_5 + Z_{16}I_{11} = 0 \tag{A.1}$$

$$Z_{61}I_1 + Z_{66}I_{11} = U_{11} \tag{A.2}$$

$$U_{11} = \left[R_{11} + R_{12} + jwL_{11} + 1/(jwC_{11}) + 1/(jwC_{12})\right]I_{11} - \left[R_{12} + 1/(jwC_{12})\right]I_1 \tag{A.3}$$

$$U_{11} = R_{11} + jwL_{11} + 1/(jwC_{11}) + (I_{11} - I_1)\left[R_{12} + 1/(jwC_{12})\right] \tag{A.4}$$